SNC--3693-5

DE87 005218

SNC-3693-5
RADIOISOTOPES AND RADIATION
APPLICATIONS
TID 4500 (55TH ED.)
UC-23

THULIUM OXIDE FUEL CHARACTERIZATION STUDY

PART I - MATERIALS PROPERTIES MEASUREMENTS

Prepared By

C. A. Nelson, R. W. Anderson, C. R. Fink,
A. Tse and W. J. Fretague

Prepared For

DIVISION OF ISOTOPES DEVELOPMENT
U.S. ATOMIC ENERGY COMMISSION

CONTRACT NUMBER: AT-(40-1)-3693

AUGUST 1970

By

SANDERS NUCLEAR CORPORATION
Nashua, New Hampshire

DISCLAIMER

TABLE OF CONTENTS

TABLE OF CONTENTS (Cont)

TABLE OF CONTENTS (Cont)

LIST OF ILLUSTRATIONS

LIST OF ILLUSTRATIONS (Cont)

SANDERS NUCLEAR CORPORATION

LIST OF TABLES

LIST OF TABLES (Cont)

ABSTRACT

A study was performed to establish the feasibility for application of encapsulated thulium-170 as an isotopic fuel for operations at temperatures to 1500°C for 180 days. Effects of various combinations of fueled capsule design parameters (fuel capsule diameters, power densities, thermal conductivities, capsule wall temperatures, fill gases and liner materials) were evaluated and compared to experimental data generated herein. A computer program was developed to predict dose rates through various thicknesses (¼, ½ and 1") of aluminum, stainless steel, lead, tungsten and depleted uranium absorbers using thermoluminescent dosimetry techniques for experimental corroboration. A basic SRL* procedure for preparing Tm_2O_3/Yb_2O_3 composites was experimentally evaluated and a modified procedure used to prepare test coupons. Melting points and solid-state transformations to the melting point of a composition series 100% Tm_2O_3 - 100% Yb_2O_3 were determined. 100% Tm_2O_3 was observed to melt at 2301 ± 33.5°C and 100% Yb_2O_3 at 2328 ± 33.5°C. The Tm_2O_3-Yb_2O_3 system remains cubic to the melting point and is typical of a solid solution system. Solid-state reaction of candidate containment materials (Hastelloy X, Hastelloy C-276, Haynes-25, T-111, TZM, tungsten and zirconium) with Tm_2O_3/Yb_2O_3 were studied. Containment for times to 10,000 hours at 1600°C and to 500 hours at 2000°C were demonstrated; no effects due to Yb_2O_3 addition were observed. The results of this study show conclusively that thulium-170 sesquioxide can be successfully applied as an encapsulated isotopic fuel.

*Savannah River Laboratory

SECTION 1
INTRODUCTION

The first thermoelectric generator was isotopically fueled more than a decade ago. That isotopes can be successfully applied in this manner is evidenced by the number of successful systems now in use. The object of this study as presented in the statement of work was "to determine the feasibility for application of encapsulated thulium-170 as an isotopic fuel for operations at temperatures up to 1500°C for 180 days. The program was conducted as a two phase study. Phase I included parametric design study of a fuel capsule, definition of property measurement procedures and evaluation of test sample preparation procedures. Phase II will be principally concerned with the measurement of thulium oxide - ytterbium oxide properties. Phase II will also include thermal testing of thulium oxide wafers produced by the Contractor's proprietary process under AEC-designated conditions and preparation of test materials."

Selection Criteria

The radiation properties of the thulium-170 are one of the bases for interest in determining the feasibility of its application as a heat source. Thulium 169 is 100% isotopically abundant and has a thermal neutron activation cross-section of 125 barns. Gamma emission (0.084 Mev) from the 128-day half-life thulium-170 is accompanied by bremsstrahlung produced from the 0.968 and 0.885 Mev beta particles. The ytterbium daughter product is stable.

Thulium metal, one possible embodiment for thulium-170, melts at 1545°C and exists as a face-centered cubic structure. The melting point

would be acceptable, although marginal, in certain applications; however, the crystal structure of the ytterbium daughter product is known to assume a close packed hexagonal arrangement and would present design limitations. In contrast, the sesquioxide is the only oxide form of thulium known to exist, and with a heat of formation (ΔH_f, 298°K.) of -451 k cal/mole[26] would be expected to exhibit great stability with respect to encapsulant material. Further, projection of existing rare earth data suggests that Tm_2O_3 would melt in excess of 2300°C and that its ytterbium daughter would also assume the sesquioxide form. However, the divalent YbO form is also known to exist and may be a factor in a feasibility of use determination.

Further support for selection of the oxide form for extensive characterization comes from experimental data that has shown that power densities of 2.4 w/gm are obtainable; hence, making Tm_2O_3 (density - 8.88 gm/cc) also a potentially useful embodiment for thermionic applications of thulium-170. Finally, the oxide is readily available in high purity with sufficient production capability existing to fulfill foreseeable future requirements.

Selection and Property Measurement

The radiation properties of thulium-170, the physical and chemical properties of the sesquioxide, its power density and availability make it a prime candidate heat source/embodiment. The course required to establish the feasibility of its application as a heat source is that developed for other past isotopes with the added benefit that a large portion of the characterization can be accomplished without using a radioactive source and all the hinderances that that entails.

The application feasibility study has been performed in two phases. Phase I dealt primarily with developing procedures to obtain data in the following property areas:

- Phase diagram of the Tm_2O_3 - Yb_2O_3 system (includes melting point determination)
- Containment materials compatibility
- Radiation dose rate and shielding design
- Fuel capsule parametric design

- Evaluation of test sample preparation procedure*

The second phase accomplished the accumulation of experimental data in accordance with established procedures and analysis thereof with respect to feasibility of application. The tasks to be performed are those singled out above. Several of the tasks are discussed in greater detail in the following topical reports:

- Compatibility Study of Containment Materials for Thulium Oxide[1]
- Phase Diagram Determination of the Tm_2O_3 - Yb_2O_3 System[2]
- Thulium Oxide Fuel Characterization Study (Thulium-170 Fueled Capsule Parametric Design)[3]
- Thulium-170 Oxide Heat Source Experimental and Analytical Radiation and Shielding Study[4]

*The authors wish to acknowledge the helpful participation of the Isotopes Development Center, Oak Ridge National Laboratories in reviewing the procedures.

SECTION 2
SUMMARY

The object of this study as presented in the Statement of Work was "to determine the feasibility for application of encapsulated thulium-170 as an isotopic fuel for operations at temperatures up to 1500°C for 180 days. The program will be conducted as a two phase study. Phase I will include parametric design study of fuel capsule, definition of property measurement procedures and evaluation of test sample preparation procedures. Phase II will be principally concerned with the measurement of thulium oxide - ytterbium oxide properties. Phase II will also include thermal testing of thulium oxide wafers produced by the Contractor's proprietary process under AEC-designated conditions and preparation of test materials."

Thulium-170 Fueled Capsule Parametric Design

Equations were developed and calculations were performed to provide temperature distribution data for individual Tm_2O_3 wafer, Tm_2O_3 bulk wafer and Tm_2O_3 microsphere encapsulations. Analytical error in the procedures developed for the wafer cases is 1% or less.

Thermal profiles are presented for power densities ranging from 8-24 w/cc with fuel capsule surface temperatures ranging from 1000-2732°F. Hastelloy-X, Haynes-25, T-222, tungsten, platinum and molybdenum liner materials are considered.

Based on thermal profile data, results show that the individual wafer encapsulation approach offers the greatest flexibility in capsule design and that of microspheres the most restrictive. Further, the

study indicates that the precision required in the investigation of the behavior of the Tm_2O_3/Yb_2O_3 system should be sufficient to detect melting within 50-100°F and that solid-state transitions, if they occur, are not expected to be a significant factor. Temperatures for compatibility tests should be well separated and accurate to ± 120°F.

The availability of several practical capsule designs for Tm_2O_3 demonstrates the feasibility of applying thulium sesquioxide as an isotopic heat source.

Thulium-170 Oxide Heat Source Experimental and Analytical Radiation and Shielding Study

Dose rates from 5, 10 and 20.7-watt Tm_2O_3 sources at two different source-to-dose point distances (19 and 100 cm) were experimentally determined using thermoluminescent dosimetry techniques. Five different absorber materials (aluminum, stainless steel, lead, tungsten and depleted uranium) of three different thicknesses (¼, ½ and 1") were used. The overall uncertainty (experimental error) in the measured dose rate was ± 9%.

A computer code (FORTRAN) was developed to generate theoretical dose rates for the uncollided flux; a buildup factor for infinite medium was used to obtain the total flux.

Predicted to measured dose rate ratios of 0.58 to 1.85 characterized results for the three most dense absorbers; ratios of 0.84 to 3.0 characterized aluminum and stainless steel. Deviations of these ratios from 1 are primarily attributable to the assumption of an infinite medium for the buildup factor in generating the theoretical dose rates. Departure of the experimental dose rates measured at 19 and 100 cm, from the inverse square relationship is attributable to the buildup factor used in the analytical predictions.

The applicability of the dose rate computational method used in this study to kilowatt sources was analyzed. It was concluded that an infinite medium buildup factor should be used and a 22 energy group computation made; dose rates accurate to 10 and 20% will result. Of equal importance to system design, required shield thicknesses (Pb, W

or U) will be overestimated by only 2 to 3%.

Test Sample Fabrication Procedure

A basic SRL process for fabricating test specimens was experimentally evaluated for applicability to the fabrication of Tm_2O_3 composite test materials. The modified process developed, can, with some quality control, reproducibly provide thulium/ytterbium oxide wafers with sintered densities to 96% of theoretical. The conversion efficiencies (oxide-to-oxide) were consistently at an acceptable 90% level or better. Coprecipitation was used to prepare the mixed oxide starting powders. The sintered wafers were homogeneous and provided a quality simulant of the radioactive fuel thereby adding to the credibility of the compatibility and phase diagram data.

Chemically reprocessed oxide did not provide any improvement in purity over the "as received" oxide. Impurities present a potential problem in that their behavioral pattern is unknown. It is recommended that other processes be studied that may be capable of providing a lower impurity level product of equally high ceramic quality.

Phase Diagram Determination of the Tm_2O_3-Yb_2O_3 System

The phase relationships of Tm_2O_3/Yb_2O_3 in a dynamic thermal environment (ambient temperature to the melting point and over the composition range 100% Tm_2O_3 - 100% Yb_2O_3) were investigated with respect to establishing the suitability of the oxide as a heat source embodiment for thulium-170.

The melting point of Tm_2O_3 (99.9%) was determined to be 2301 ± 33.5°C and that of Yb_2O_3 to be 2328 ± 33.5°C using zirconia (calcia stabilized) containers in an argon atmosphere. No solid-state phase transformations were observed from ambient temperature to the melting point.

A phase diagram of the Tm_2O_3/Yb_2O_3 system was determined for the entire composition range and is typical of a solid solution system. Additional data supporting a solid solution system was derived from both metallographic and x-ray diffraction measurement of samples exposed to temperatures up to 2000°C for periods up to 4000 hours.

Experimental determination of the melting point of high purity aluminum oxide (Al_2O_3) was used to standardize the phase diagramming apparatus; a system error of + 20°C was determined and the experimental data corrected accordingly.

Compatibility Study of Containment Materials for Thulium Oxide

The compatibility of Tm_2O_3 and Tm_2O_3/Yb_2O_3 containing up to 20% Yb_2O_3 was determined with seven candidate encapsulant materials. Determination of compatibility was based on the following:

- Penetration of Tm_2O_3/Yb_2O_3 into the encapsulant material.
- Penetration of the encapsulant material into the Tm_2O_3/Yb_2O_3.
- Structural changes in the thulia.
- Physical changes in the thulia.

Evaluations were performed by visual and metallographic examination, x-ray diffraction, x-ray fluorescence and electron microprobe analyses. A summary of the evaluations is given in Table 4-1. (The Yb_2O_3 content of the thulia showed no significant effect with respect to compatibility with the container materials, hence the Yb_2O_3 content is not shown as a variable.) The instrumental analyses were performed at a qualitative level to identify major effects; more detailed analyses were beyond the scope of this study.

Comparison of the compatibility of thulia prepared by two processes showed no difference in compatibility with respect to the encapsulant material. However, the behavior of the thulia was different for the two processes as indicated by the tendency toward translucence and toward modification in its crystalline structure after tests at 1600°C and 2000°C. The difference in behavior was believed to be due, at least in part, to the impurity content of the thulia.

Based on the test data obtained from this study, it was concluded that Tm_2O_3/Yb_2O_3 can be successfully contained under the following conditions:

Container Material	Time, Hours	Maximum Temperature, °C
Hastelloy-X	10,000	1000
Haynes-25	10,000	1000
T-111	10,000	1600
TZM	10,000	1600
	500	2000
Tungsten	10,000	1600
	500	2000
Zirconium	6,500	600
	Conditional Application over 500 hours	1000
Hastelloy C-276	6,500	1000

The above encapsulant conditions are conservative since at these conditions no penetration of the encapsulant material was observed. Selection of specific encapsulant materials would be determined by system design and mission requirements. The demonstrated compatibility of the seven encapsulant materials with thulia provide considerable latitude to the system designer in encapsulant selection.

Although the Tm_2O_3/Yb_2O_3 did not enter the container materials during the various test cycles, some changes in the Tm_2O_3/Yb_2O_3 were observed. The mechanisms causing these changes were not known and their study was beyond the scope of this program. Observed changes in the oxide discs were:

- Slight powdering of the oxide after testing in Hastelloy-X at 600 and 1000°C and in T-111 at 1000°C.
- Increase in coloration of the oxide with increasing severity of tests.
- Change in crystalline structure of Tm_2O_3 (SNC Process) after testing with tungsten at 1600 and 2000°C, and Tm_2O_3 (SRL Process) with zirconium at 1000°C.
- Increase in degree of transparency to visible light with increasing severity of heat treatment of Tm_2O_3 tested in Haynes-25, Hastelloy-X, and tungsten.

- Decrease in degree of transparency to visible light with increasing severity of heat treatment for Tm_2O_3 tested in T-111, TZM, Zirconium and Hastelloy C-276.

Although these changes were observed in the Tm_2O_3, they do not pose restriction on the application of Tm_2O_3 as a heat source except possibly in those applications where mechanical stability of the fuel is specified.

The results show the properties of thulium oxide to be in good agreement with projected behavior and conclusively demonstrate that thulium-170 sesquioxide can be successfully applied as an encapsulated isotopic fuel for operations at temperatures to 1500°C and be successfully contained for times through 180 to 420 days.

SECTION 3
Tm_2O_3/Yb_2O_3 PHASE DIAGRAM

3.1 INTRODUCTION

The candidacy of a radionuclide as a heat source is based not only on its nuclear properties, but also on the chemical and physical characteristics of the form in which the nuclide will be embodied.

Thulium-170 has nuclear properties that make it desirable as a heat source; the oxide of thulium has physical characteristics that are expected to be superior to the metal with respect to its utilization as a heat source embodiment. However, the real potential of thulium oxide cannot be fully assessed until the limits of its operational use are defined; knowledge of the Tm_2O_3/Yb_2O_3 phase diagram is essential to this assessment of operational potential, as ytterbium is the decay product of thulium.

The purpose of this study has been to characterize the Tm_2O_3/Yb_2O_3 system according to solid-state phase transformations and melting temperatures.

3.2 MELTING POINT DETERMINATION

Samples covering the full range of composition (100% Tm_2O_3 - 100% Yb_2O_3) were thermally analyzed by inductively heating the samples in an argon atmosphere and recording the temperature profiles as they were cycled through the melting point. Calcia stabilized zirconia was used as the containment for the powder and a tungsten crucible as the susceptor. Details on the fabrication of samples, certification of material and phase diagram apparatus including susceptor, are found in SNC-3693-2[2].

Initial thermal arrests were obtained from the heating curves. The melting points are given below in Table 3-1 and are corrected for systemic error. (See 3.5, Standardization.)

TABLE 3-1

MELTING POINTS (CORRECTED*) OF Tm_2O_3/Yb_2O_3 OVER THE RANGE 100% Tm_2O_3 - 100% Yb_2O_3

Composition (Tm_2O_3/Yb_2O_3)	Melting Points, °C
100/0	2257, 2281, 2295
90/10	2313, 2346, 2375
70/30	2277, 2294, 2311
50/50	2289, 2335, 2339
30/70	2255, 2290, 2315
10/90	2360, 2361
0/100	2309, 2341

Initial thermal arrests could be observed in almost all test runs. However, further analysis of the heating curves in some case proved difficult in that termination of the initial arrest could not be clearly identified and in other cases more than one thermal arrest was observed. (See Table 3-2 for experimental data.) Although the samples had wetted the sides of the containment vessel, metallographic investigations of selected samples showed that incomplete melting had taken place and that a second phase[5] was present indicating a reaction after initial melting. These factors made it difficult to interpret the terminal arrest data of the heating curves and, because of the alloying effect, any of the arrest data of the cooling curves with respect to establishing the melting point. Therefore, only the initial thermal arrests of the heating curves have been considered.

The melting point of each of the members has been obtained by treating the data in Table 3-1 in a least squares manner, calculating the melting point of the end members from the least squares relation-

*Reference - Al_2O_3 obtained from the National Bureau of Standards.

TABLE 3-2

EXPERIMENTAL DATA - THERMAL ANALYSIS (100% Tm_2O_3 - 100% Yb_2O_3)

Sample No.	Composition	1st Arrest Start	1st Arrest End	Time	2nd Arrest Start	2nd Arrest End	Time
PD3	100/0	2300	2320	3'00"			
PD4	100/0	--	--	--			
PD5	100/0	2314	2340	2'50"			
PD6	100/0	2276	2297	2'50"			
PD7	0/100	2328	2362	3'21"			
PD8	0/100	?					
PD9	0/100	?			?		
PD26	0/100	2360	2366	2'00"	2380	?	?
PD10	50/50	2308	?				
PD11	50/50	2360	2368	1'30"			
PD12	50/50	2354	?				
PD13	70/30	2313	?				
PD14	70/30	2330	2356	4'00"			
PD15	70/30	2296	2318	2'12"	2332	?	?
PD16	30/70	2334	2359	2'36"	2374	2386?	1'06"?
PD17	30/70	2309	2343?	3'15"?	?		
PD18	30/70	2274	2280	1'30"	?		
PD19	30/70	?					
PD20	90/10	2394	2394	2'15"			
PD21	90/10	2366	?	?			
PD22	90/10	2332	?	?			
PD23	10/90	?					
PD24	10/90	2380	2393	3'30"			
PD25	10/90	2379	2416	3'20"			
C1	100% Al_2O_3	2050	?				
C2		--					
C3		--					
C4		2074	?				
C5		2110	2114	2'03"			
C6		2068	2076	2'00"			
C6A		2028	2054	1'41"			
C7		2030	2057	1'48"			
C8		2084	2104	3'41"			
C9	100% Al_2O_3	2075	2082	2'13"			

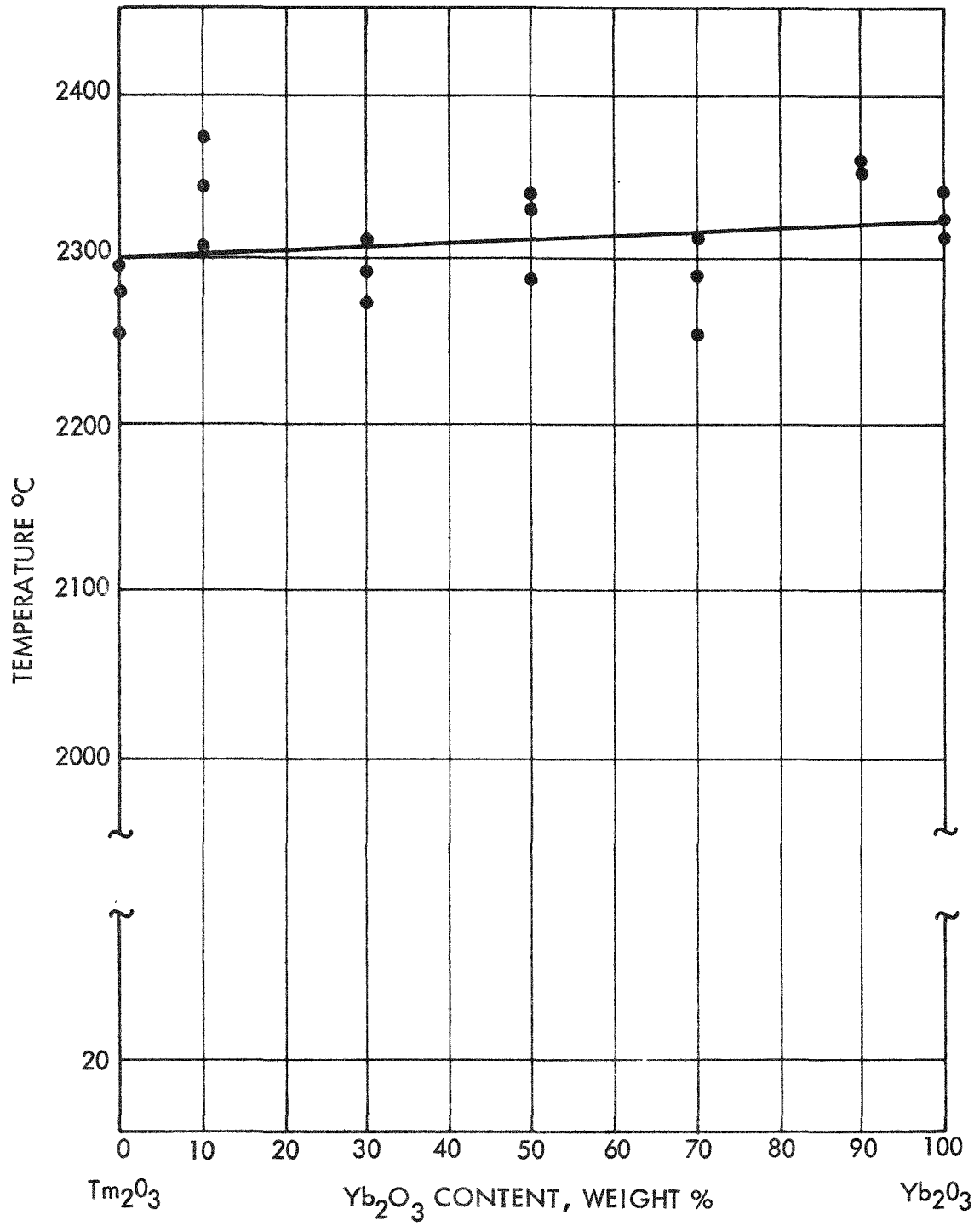

Figure 3-1. Phase Diagram Tm_2O_3 - Yb_2O_3

ship and then establishing the melting point of the other compositions. The results given in Table 3-3 are obtained from the plot of the least squares data shown in Figure 3-1.

TABLE 3-3

MELTING POINTS OF Tm_2O_3/Yb_2O_3 OVER THE RANGE 100% Tm_2O_3 - 100% Yb_2O_3

Composition (Tm/Yb)	Melting Points, ^{o}C
100/0	2301
90/10	2303
70/30	2308
50/50	2312
30/70	2316
10/90	2321
0/100	2328

The deviation of these points at the 1σ level is ± 33.5^{o}C.

3.3 SOLID-STATE TRANSFORMATIONS

No experimental evidence was obtained that indicated a solid-state phase transformation had occurred between ambient temperature and the melting point. This finding was substantiated by metallographic investigation of several samples in the composition range 100% Tm_2O_3 - 80/20% Tm_2O_3/Yb_2O_3 that had experienced temperatures of 600, 1000, 1600 and 2000^{o}C for up to 4000 hours. The data also indicated that Tm_2O_3-Yb_2O_3 formed stable solid solutions at all compositions.

In addition, x-ray diffraction analysis of samples treated at 600, 1000, 1600 and 2000^{o}C for up to 2500 hours in the same composition range, showed no evidence of solid-state transformation and again indicated that Tm_2O_3 and Yb_2O_3 were mutually soluble in the solid state.

3.4 PHASE DIAGRAM

Figure 3-1 shows the phase diagram over the composition range from 100% Tm_2O_3 to 100% Yb_2O_3 as constructed from a least squares fit of the Table 3-1 data. The data points shown are those listed in Table 3-1 and fall within ± 33.5^{o}C of the curve at the 1σ

confidence level. The diagram shows the melting point of pure thulia to be 2301 ± 33.5°C and that of pure ytterbia to be 2328 ± 33.5°C. The shape of the curve is typical of a solid solution system. It is assumed that the liquidus curve was near the solidus curve and that both fell within the experimental band.

3.5 STANDARDIZATION

Standardization of the system was accomplished by treating several samples of high purity aluminum oxide[6] (Al_2O_3) in a manner similar to that used in the thulia/ytterbia tests. The experimental data obtained appears in Table 3-2.

The average melting point obtained for the alumina was 2065 ± 27°C. The melting point reported by Schneider and McDaniel[7] is 2045 ± 6°C for an identical Al_2O_3 sample in an argon atmosphere on a tungsten hearth plate. A comparison of these results indicates a system error of + 20°C. On this basis, all experimentally observed points were adjusted downward by this amount.

3.6 DISCUSSION

The melting points observed in this work are somewhat lower than those observed by other investigators. Smith[8] reports a melting point of 2377 ± 100°C for Tm_2O_3 using a Mendenhall V filament furnace. ORNL[9] has determined the melting point of Yb_2O_3 to be 2385°C, while Eyring and Eick[10] report a melting point of 2346°C and Rohden[11], 2350°C. The temperatures observed in our experiments and those reported herein are sufficiently close in agreement as to recommend them as reliable melting points.

The end members have been investigated with respect to solid-state phase transformation[12][13][14][15][16][17]. All report the C-type (cubic) structure to be the only existent phase for both Tm_2O_3 and Yb_2O_3 except M. Fŏéx and J. P. Traverse[17]. Using high temperature x-ray diffraction analysis, they observed a transition from C-type to A-type in Tm_2O_3 at 2280°C. Our

experiments gave no indication of any solid-state phase transformations in any of the compositions studied.

SECTION 4
COMPATIBILITY STUDY OF CONTAINMENT MATERIALS FOR THULIUM OXIDE

4.1 INTRODUCTION

Successful application of Tm_2O_3 as a high temperature isotopic heat source requires materials compatibility between the Tm_2O_3 and the primary encapsulant. To determine the compatibility of Tm_2O_3 with seven candidate encapsulant materials, a series of long-term tests were designed, performed and evaluated. The test parameters included in the evaluation were:

- Encapsulant materials -- Hastelloy-X, Haynes 25, T-111, TZM, tungsten, Hastelloy C-276 and zirconium.
- Thulia composition -- Tm_2O_3 containing 0, 5, 10 and 20% Yb_2O_3 (Yb is the decay product of Tm-170).
- Temperatures -- 600, 1000, 16000 and 2000°C.
- Time -- 500, 2500, 4000, 6500 and 10,000 hours.
- Procedure of Tm_2O_3 processing -- "Savannah River Laboratory (SRL)" and "Sanders Nuclear Corporation (SNC)" processes.

To properly evaluate "compatibility" requires definition of several aspects wherein incompatibility could be measured or observed. In this study, four aspects of incompatibility were defined.

1. Depth of penetration of the thulia and/or ytterbia into the encapsulant material.
2. Depth of penetration of encapsulant components into the thulia.

3. Structural changes in the thulia, i.e., cracking, powdering, etc.

4. Physical changes in the thulia, i.e., coloring, translucency and phase modification.

Determination of the type and degree of incompatibility was performed by visual and metallographic examination, and, x-ray diffraction, x-ray fluorescence, and electron microprobe analyses. These analyses yielded several interesting observations in addition to compatibility data; a full understanding of these was not developed since study beyond recording of the observations was outside the scope of the current program. A listing of the compatibility samples examined, methods of analysis employed and the results of visual observation is given in Section 4.9.2.

Details of samples preparation and test procedures are contained in SNC-3693-1[1]. Briefly, the samples were prepared by the SRL process[18] and the SNC process, a proprietary process developed independently by Sanders Nuclear Corporation. The test capsules were heavy-walled containers of the test metal containing a single thulia disc between discs of the test metal. The containers were vacuum-sealed by electron beam welding, thereby providing a closed-reaction system. In addition to the test samples, control samples were prepared. The controls consisted of three thulia discs, vacuum-sealed in containers so that the middle thulia disc was not in direct contact with the metal sample.

Detailed evaluation of the majority of the compatibility samples were previously reported in SNC-3693-1. In the following sections, this prior data is briefly summarized and the additional data presented in detail. The final sections contain a summary of the total data.

4.2 COMPATIBILITY OF HASTELLOY X - Tm_2O_3 - Yb_2O_3

4.2.1 SUMMARY OF PRIOR TESTS

The evaluation of the compatibility of Hastelloy X with Tm_2O_3/Yb_2O_3 was reported previously in Section 3 of report SNC-3693-1. The test conditions were:

Tm_2O_3 composition:	Tm_2O_3 with 0, 5, 10 and 20% Yb_2O_3.
Temperature:	600 and 1000°C
Times:	500, 2500 and 4000 hours
Atmosphere:	static vacuum (sealed capsule)

The results of this evaluation are summarized as follows:

1. No bonding was observed at the Hastelloy-X - Tm_2O_3 interface after 4000 hours at 600 and 1000°C.

2. The Hastelloy-X was not attacked or penetrated by the Tm_2O_3 after 4000 hours at 600 and 1000°C.

3. The component elements of the Hastelloy-X did not penetrate the Tm_2O_3 after 4000 hours at 1000°C. However, some transference of iron to the oxide surface was detected after 2500 hours at 1000°C.

4. The Tm_2O_3 showed some surface degradation in the form of intergranular attack after 2500 hours at 1000°C. It was postulated that this attack was caused by some component of the Hastelloy-X.

5. Yb_2O_3 additions of 5, 10 and 20% to Tm_2O_3 had no effect on the compatibility of the Hastelloy-X - Tm_2O_3 system.

4.2.2 EVALUATION OF 10,000-HOUR TESTS

As compared with the 4000-hour tests at 600 and 1000°C, testing to 10,000 hours caused no further change in the appearance of the Hastelloy-X - Tm_2O_3 specimens. The materials showed no evidence of bonding at the interface and the Hastelloy-X was unaffected by the Tm_2O_3 (Figures 4-1 through 4-3). The Tm_2O_3 tested at 1000°C showed some evidence of surface attack in the form of intergranular attack and powdering but to approximately the same degree observed at 4000 hours of testing. The Tm_2O_3 tested at 600°C was apparently unaffected by the increased exposure time. X-ray diffraction analysis revealed only the Tm_2O_3 structure. Electron microprobe analysis detected no penetration of Tm or Yb into the Hastelloy-X. Of the elements contained in Hastelloy-X,

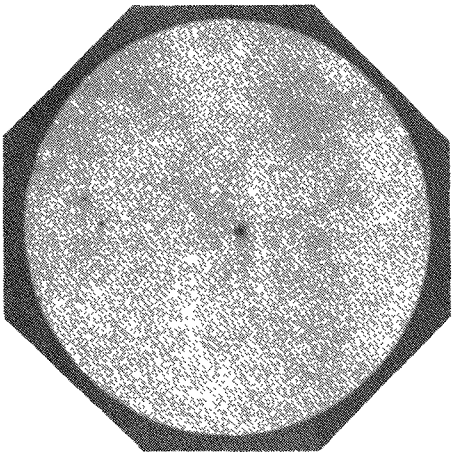

a. 100% Tm_2O_3 (SRL)

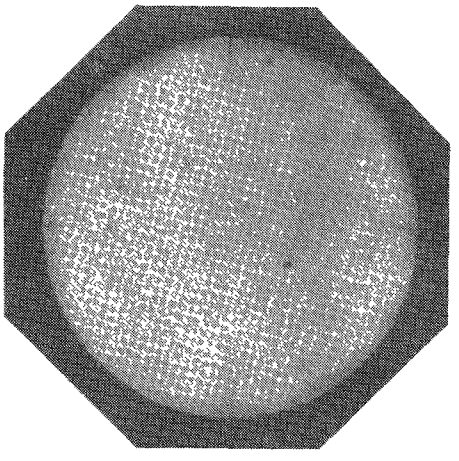

b. 80% Tm_2O_3 - 20% Yb_2O_3 (SRL)

Figure 4-1. Thulia Tested 10,000 Hours at 600°C with Hastelloy-X

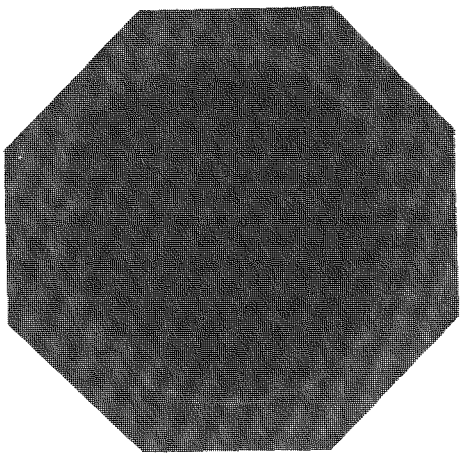

a. 80% Tm_2O_3 - 20% Yb_2O_3

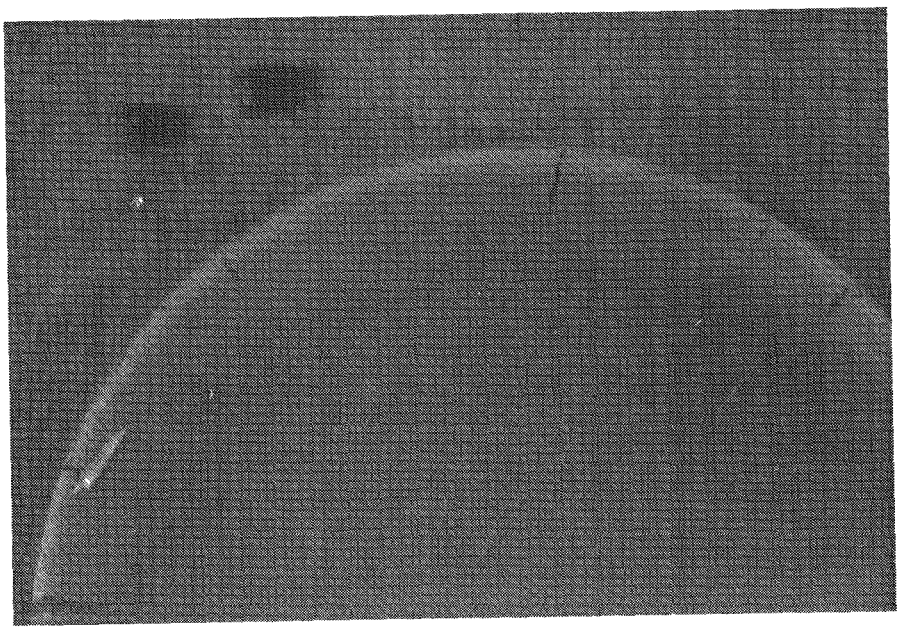

b. Same as a. Note granular appearance at radial cracks.

Figure 4-2. Thulia Tested 10,000 Hours at 1000°C with Hastelloy-X

a. 600°C Test

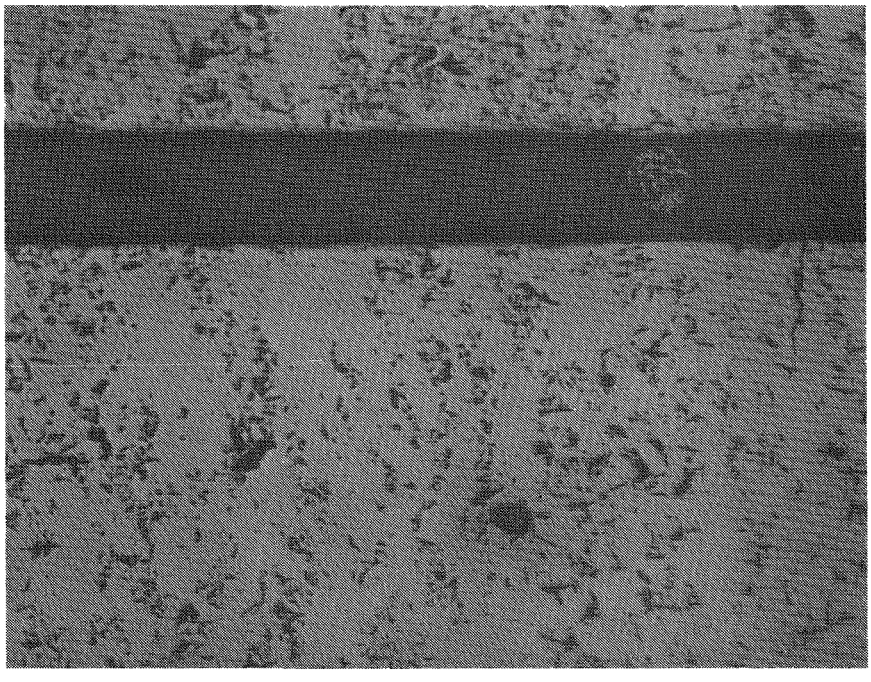

b. 1000°C Test

Figure 4-3. Micrographs of 80% Tm_2O_3 - 20% Yb_2O_3 after 10,000 Hours with Hastelloy-X. 100X.

only Cr and Fe were found in the Tm_2O_3 when tested at 1000°C; the Cr was found only near the surfaces of the oxide wafer but the Fe had permeated the disc. Approximate concentrations within the 0.06 inch thick wafers were:

	Surface of Wafer	Center of Wafer
Cr	0.05%	none detected
Fe	0.08%	0.02%

The addition of 5, 10 and 20% Yb_2O_3 to Tm_2O_3 had no observable effect on the compatibility of the Hastelloy-X - Tm_2O_3 system.

4.2.3 ASSESSMENT OF HASTELLOY-X - Tm_2O_3 COMPATIBILITY*

The test data has shown that Tm_2O_3 containing to 20% Yb_2O_3 can be successfully contained in Hastelloy-X at temperatures to 1000°C and for times to 10,000 hours. Since the Hastelloy-X was not attacked or penetrated by the Tm_2O_3, minimum containment thickness would be selected based on other requirements such as environmental corrosion resistance or structural strength. The Tm_2O_3 exhibited fair structural stability within the Hastelloy-X, notwithstanding some cracking and surface powdering. There was no evidence of swelling or phase transformations of the oxide.

4.3 COMPATIBILITY OF HAYNES-25 - Tm_2O_3/Yb_2O_3

4.3.1 SUMMARY OF PRIOR TESTS

The evaluation of Haynes-25 with Tm_2O_3/Yb_2O_3 was reported in Section 4 of report SNC-3693-1. The test conditions were:

Tm_2O_3 composition:	Tm_2O_3 with 0, 5, 10 and 20% Yb_2O_3.
Temperature:	600 and 1000°C.
Times:	500, 2500 and 4000 hours.
Atmosphere:	static vacuum (sealed capsules)

The results of the evaluation are summarized below:

1. No bonding occurred between the Haynes-25 and the Tm_2O_3 after 4000 hours at either 600 or 1000°C.

*See also Section 4.8.3, p. 4-36 "Assessment of the Compatibility of Hastelloy C-276 with Tm_2O_3."

THIS DOCUMENT CONTAINS PROPRIETARY INFORMATION OF SANDERS NUCLEAR CORP., AND IS TO BE USED ONLY FOR THE PURPOSE FOR WHICH IT HAS BEEN SUPPLIED. THIS DOCUMENT IS NOT TO BE DUPLICATED IN WHOLE OR IN PART WITHOUT PRIOR WRITTEN PERMISSION FROM A DULY AUTHORIZED REPRESENTATIVE OF THE SANDERS NUCLEAR CORP

2. The Haynes-25 was not attacked or permeated by the Tm_2O_3 after 4000 hours at either 600 or 1000°C.

3. No components of the Haynes-25 attacked or permeated the Tm_2O_3.

4. The Tm_2O_3 exhibited excellent structural stability when contained in Haynes-25 for times to 4000 hours and temperature to 1000°C. Whereas some cracking of the oxide was observed, the cause was not attributable to any reaction with Haynes-25.

5. Yb_2O_3 additions of 5 and 10% to the Tm_2O_3 had no effect on the compatibility of Haynes-25 - Tm_2O_3.

4.3.2 EVALUATION OF 10,000-HOUR TESTS

The increased exposure at 600 and 1000°C to 10,000 hours caused no changes in the appearances of either the Tm_2O_3 or the Haynes-25. Visual examination showed no indications of bonding reaction, or mass transport within the capsule (Figures 4-4 and 4-5). The oxide wafers were grey/green in color and contained some cracks; the degree of coloration and cracking were similar to that observed after 4000 hours exposure. The surface of the oxide wafers appeared granular suggesting grain growth and thermal etching of the grain boundaries. A slight amount of powdering of the oxide was observed on some samples but due to the difficulty in detecting small quantities of powder on the oxide surfaces, it was assumed all samples experienced at least some powdering.

X-ray diffraction analysis of the Tm_2O_3 after 10,000 hours at 600 and 1000°C revealed only the Tm_2O_3 crystalline structure; there was no evidence of instability or formation of some reactant product.

Electron microprobe analysis detected the transfer of Cr and Co from the Haynes-25 to the thulia. Approximate concentrations were:

	Near Surface of Tm_2O_3 Wafer	Center of Tm_2O_3 Wafer
10,000 hours - 600°C		
Cr	0.2 - 0.4%	0.02%

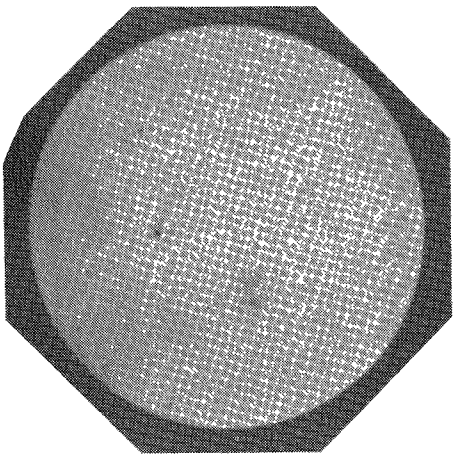

a. 100% Tm_2O_3 (SRL)

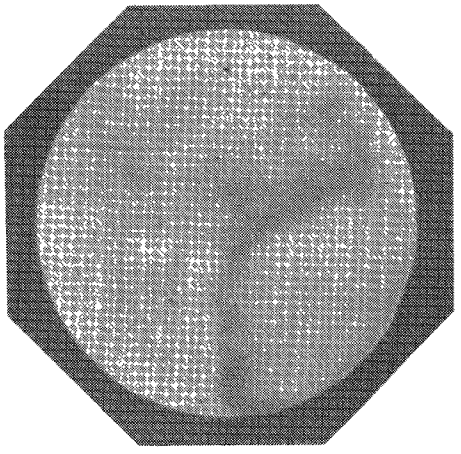

b. 90% Tm_2O_3 - 10% Yb_2O_3 (SRL)

Figure 4-4. Thulia Tested 10,000 Hours at 600°C with Haynes-25

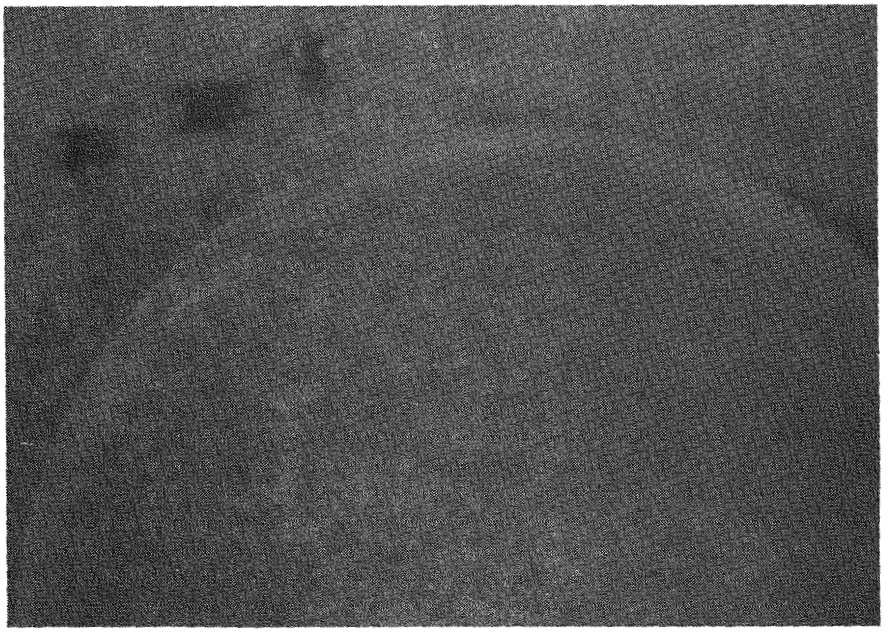

a. 100% Tm_2O_3 (SRL)

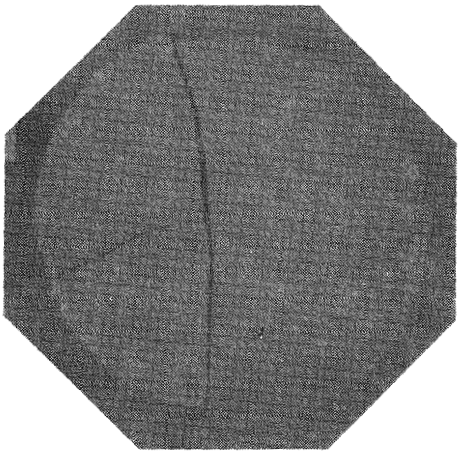

b. 90% Tm_2O_3 - 10% Yb_2O_3 (SRL)

Figure 4-5. Thulia Tested 10,000 Hours at 1000°C with Haynes-25

Co	0.15%	0.05%

10,000 hours - 1000°C

Cr	0.02%	0.01%
Co	0.1 - 0.3%	0.05%

Other constituents of the Haynes-25 were not detected in the thulia. Likewise, neither Tm nor Yb were detected within the Haynes-25.

Microscopic examination of the Haynes 25 specimens showed no evidence of attack or reaction with the thulia after either the 600°C or 1000°C treatment (Figure 4-6). The 1000°C specimens did show some depletion of the grain boundary phase to a depth of about 0.01 inch below the surface of the thulia interface. Apparently, this phase depletion was related to the transport of Cr to the thulia.

There was no evidence that additions of 5 and 10% Yb_2O_3 to the thulia affected in any way the compatibility of Haynes-25 - Tm_2O_3.

4.3.3 ASSESSMENT OF HAYNES-25 - Tm_2O_3 COMPATIBILITY

Compatibility tests have demonstrated that Tm_2O_3 can be successfully contained for at least 10,000 hours at temperatures to 1000°C. Since the Haynes 25 neither reacted nor was penetrated by Tm, design of containment capsules would not be restricted by compatibility considerations at use temperatures to 1000°C. Tm_2O_3 containing to 20% Yb_2O_3 proved to be structurally stable and compatible with Haynes-25 at temperatures to 1000°C.

4.4 COMPATIBILITY OF T-111 - Tm_2O_3/Yb_2O_3

4.4.1 SUMMARY OF PRIOR TESTS

The results of the evaluation of the compatibility of the T-111 - Tm_2O_3 system were reported in Section 5 of report SNC-3693-1. The test conditions were:

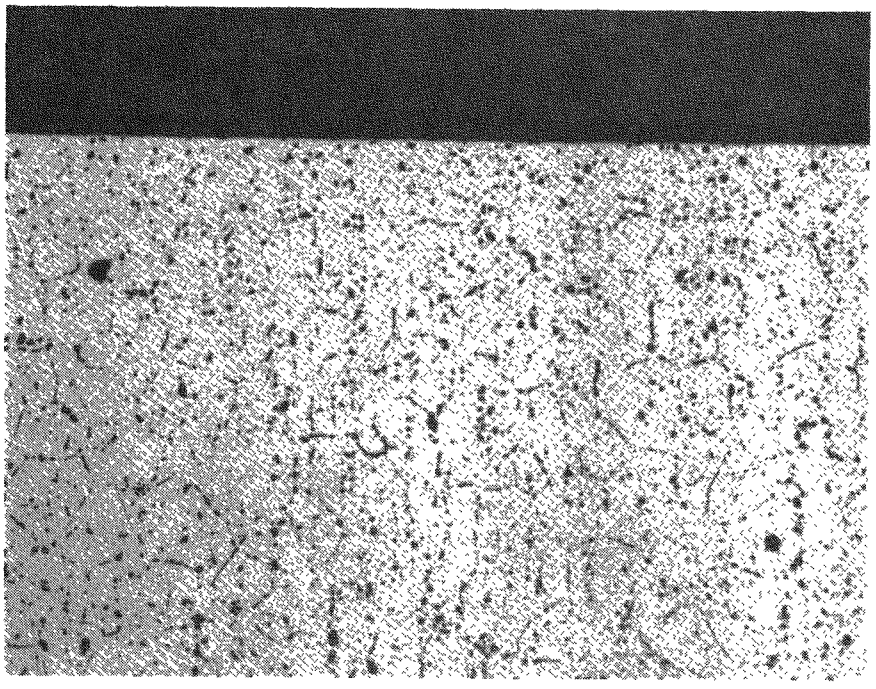

a. Haynes-25

b. 90% Tm_2O_3 - 10% Yb_2O_3 (SRL)

Figure 4-6. Micrographs of Haynes-25/Thulia after 10,000 Hours at 1000°C. 100X.

Tm_2O_3 composition:	Tm_2O_3 with 0, 5, 10 and 20% Yb_2O_3
Temperature:	1000 and 1600°C
Times:	500, 2500 and 4000 hours
Atmosphere:	static vacuum (sealed capsules)

The results of the evaluation are summarized below:

1. Tests at 1000°C for times to 4000 hours resulted in T-111 - Tm_2O_3 interaction in the form of
   - slight bonding
   - powdering of the Tm_2O_3
   - moderate cracking of the Tm_2O_3
   - transference of trace amount of Hf from the T-111 to the Tm_2O_3.
2. Tests at 1600°C for times to 4000 hours resulted in similar interaction as above but to a greater extent.
3. Tests at both 1000 and 1600°C resulted in no detectable attack or infusion of the T-111 by the Tm_2O_3.
4. Addition of 5, 10 and 20% Yb_2O_3 to the Tm_2O_3 had no apparent effect on the compatibility of the T-111 - Tm_2O_3 system.

4.4.2 EVALUATION OF 10,000-HOUR TESTS

The 10,000-hour tests at 1000°C resulted in similar behavior compared with the tests to 4000 hours. The T-111 was not attacked and did not show evidence of reaction (Figures 4-7a and 4-8a). Neither Tm nor Yb was detected in the T-111 by microprobe analysis. Likewise the Tm_2O_3 was not attacked and appeared unaffected by the increased test period. X-ray diffraction analysis showed only the Tm_2O_3 structure.

Unlike the 1000°C tests, the 10,000 hour test at 1600°C resulted in gross reaction of the Tm_2O_3 and moderate reaction of the T-111 (Figures 4-7b and 4-8b). The Tm_2O_3 contained a 0.004 inch thick surface layer that appeared glassy and brown. The layer was easily removed by chipping and the substrate material was the typical grey/green color of thulia. X-ray diffraction analysis

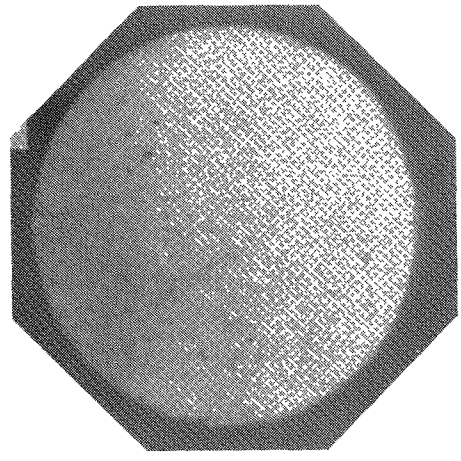

a. 100% Tm_2O_3 after 1000°C Test

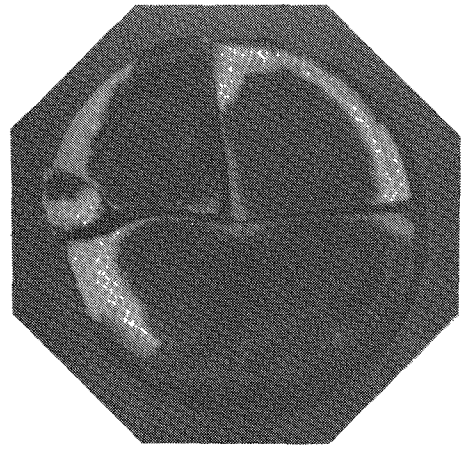

b. 90% Tm_2O_3 - 10% Yb_2O_3 after 1600°C. Test.

Note brown surface layer and light substrate.

Figure 4-7. Thulia Tested 10,000 Hours with T-111

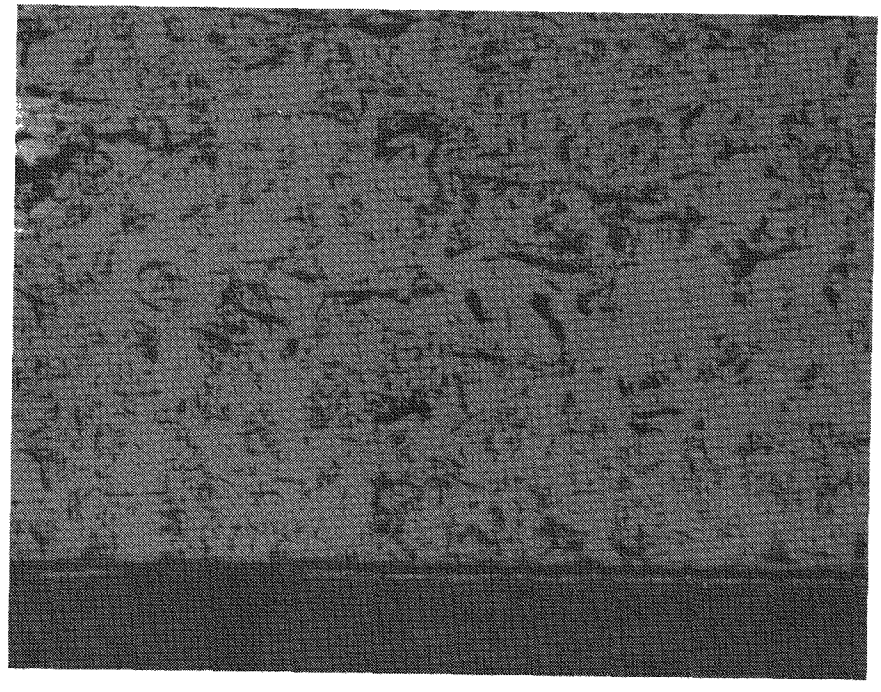

a. 90% Tm_2O_3 - 10% Yb_2O_3 after 1000°C Test

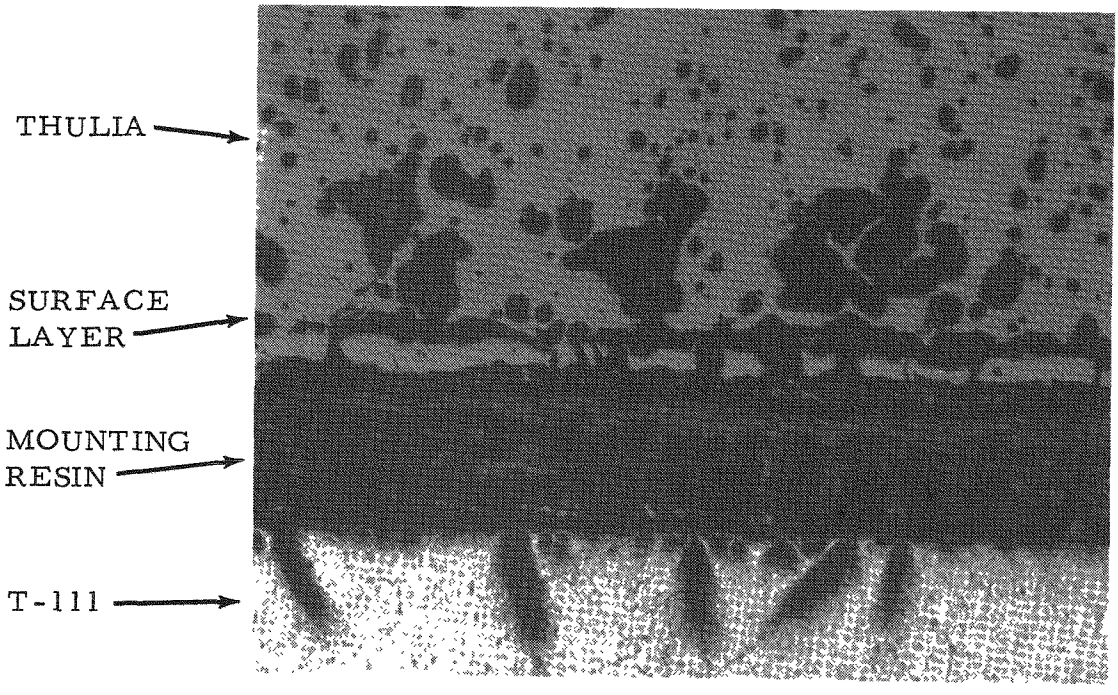

b. 90% Tm_2O_3 - 10% Yb_2O_3 after 1600°C Test

Note surface reaction layer and porosity in thulia and grain boundary attack in T-111

Figure 4-8. Micrographs of Thulia after 10,000-Hour Tests with T-111. 100 X.

of the brown layer indicated the material was at least partially crystalline, but was no longer Tm_2O_3; the identity of the brown layer could not be determined. The brown layer contained approximately 40% Ta and a small quantity of Hf as well as Tm and Yb as determined by electron microprobe analysis. Microscopic examination of the thulia clearly showed the brown layer as well as porosity extending about 0.015 inch below the surface. The T-111 also experienced some attack along the grain boundaries to a depth of about 0.007 inch and generally along the surface to a depth of about 0.002 inch. Electron microprobe analysis detected neither Tm nor Yb in the T-111 so that the identity of the elements affecting the T-111 remain undetermined (however, oxygen would be the most likely contaminant).

4.4.3 ASSESSMENT OF T-111 - Tm_2O_3 COMPATIBILITY

At temperatures to 1000°C, T-111 was sufficiently compatible with Tm_2O_3 for times to 10,000 hours to the extent that the T-111 was not detectably attacked or permeated by Tm. However, some degradation of the thulia was observed in the form of cracking and powdering.

At 1600°C, both the T-111 and the Tm_2O_3 experienced sub-surface reactions between the 4000 to 10,000 hour time period. The observed grain boundary attack in the T-111 is considered particularly serious insofar as it would be expected to cause significant reduction of mechanical properties. The formation of the unidentified brown layer on the thulia presents a potential problem in that the chemical and physical properties are unknown.

4.5 COMPATIBILITY OF TZM - Tm_2O_3/Yb_2O_3

4.5.1 SUMMARY OF PRIOR TESTS

The evaluation of the compatibility of TZM with Tm_2O_3 was reported previously in Section 6 of SNC-3693-1. The test conditions were:

Tm_2O_3 composition	Tm_2O_3 with 0, 5, 10 and 20% Yb_2O_3.

Times at temperature:	500, 2500 and 4000 hours at 1600°C
	500 hours at 2000°C
Atmosphere:	static vacuum (sealed capsules).

The results of this evaluation are summarized as follows:

1. Some bonding of the TZM and thulia occurred after the 1600 and 2000°C tests. However, the interaction was limited to the surfaces of both materials. After 4000 hours at 1600°C, no infusion of the TZM was detected in thulia and no Tm nor Yb was detected in the TZM. After 500 hours at 2000°C, only Ti (from the TZM) infused into the thulia; and neither Tm nor Yb infused into the TZM.

2. The TZM showed no evidence of attack after 4000 hours at 1600°C nor after 500 hours at 2000°C.

3. Exposures at either 1600 or 2000°C caused no detectable change in the crystalline structure of the Tm_2O_3.

4. The surface of the thulia contained coarse grains of Tm_2O_3 - the size and perfection of the crystals suggested some vapor phase growth.

5. The thulia wafers suffered only slight cracking and showed no evidence of powdering.

4.5.2 EVALUATION OF 10,000-HOUR TESTS

The most obvious effect of the 10,000-hour test at 1600°C was that Tm_2O_3 had vapor transported to the TZM capsule surfaces. The Tm_2O_3 deposit was concentrated on the bottom portion of the capsule; presumably the capsule contained a thermal gradient and the deposit concentrated at the cooler region. The deposited crystals were nearly perfect polygons ranging in size to several mils and were tightly bonded to the TZM (Figure 4-9). The crystalline structure of the deposit was that of Tm_2O_3 as determined by x-ray diffraction analysis. The Tm/Yb ratio of the deposit was 9 as determined by electron microprobe analysis; the composition of the deposit was essentially the same as the starting compositions of the wafer 90% Tm_2O_3 + 10% Yb_2O_3. Apparently, the Tm_2O_3/Yb_2O_3

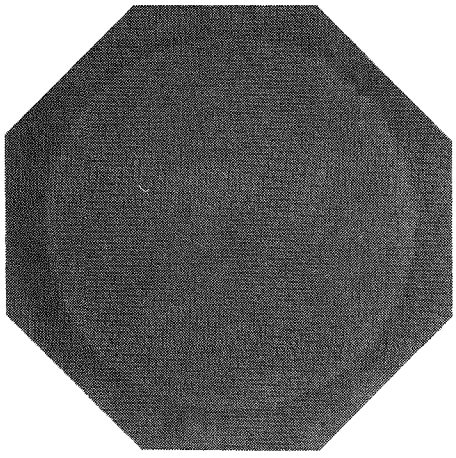

a. 90% Tm_2O_3 - 10% Yb_2O_3 Wafer (SRL)

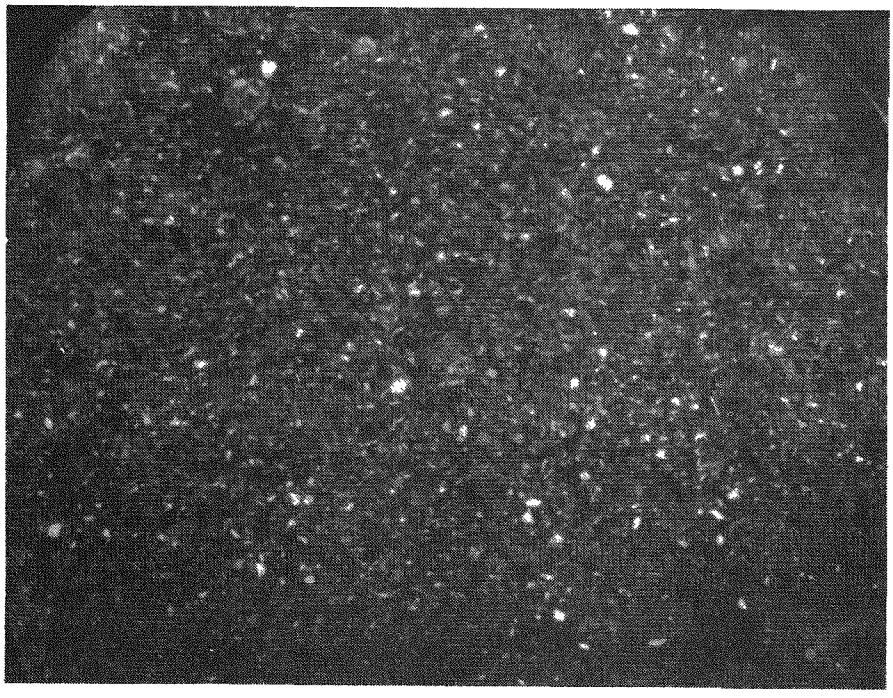

b. Thulia Crystals Vapor Deposited on TZM Capsule

Figure 4-9. Thulia Tested 10,000 Hours at 1600°C

vaporized as a true solution. As determined by microscopic and electron microprobe analysis, the reaction between the Tm_2O_3 deposit and the TZM was limited to the surface - no evidence of reaction or infusion of Tm or Yb was detected.

The surface of the oxide was irregular as if vaporization had been selective along some boundaries (Figure 4-10). The depth of the surface irregularities ranged to about 6 mils. No infusion of Mo, Ti or Zr was detected by electron microprobe analysis nor was their any direct reaction with the TZM. The oxide wafer was not cracked after the 10,000-hour exposure at 1600°C.

4.5.3 ASSESSMENT OF THE TZM - Tm_2O_3 COMPATIBILITY

The TZM - Tm_2O_3 system has demonstrated excellent compatibility for times to 10,000 hours at 1600°C and 500 hours at 2000°C insofar as direct interaction and permeation of the TZM by Tm. Since no detectable attack at the TZM interface was detected (limit of detection about 1 micron), the thickness of a TZM container could be minimal and would be determined by structural specifications. The Tm_2O_3 exhibited compatibility at 1600 and 2000°C in that the Tm_2O_3 crystalline structure was unaltered and there was no evidence of reaction with any component of the TZM. The mass transfer of the Tm_2O_3 to the TZM is believed to be a vapor transport mechanism. It could not be determined if the TZM enhanced the vapor transport of the Tm_2O_3 but as discussed in the following section, similar behavior was observed for Tm_2O_3 contained in tungsten. The material that was vapor transported retained the Yb_2O_3 concentration of the oxide wafer.

4.6 COMPATIBILITY OF TUNGSTEN - Tm_2O_3/Yb_2O_3

4.6.1 SUMMARY OF PRIOR TESTS

The evaluation of the compatibility of tungsten with Tm_2O_3 was reported previously in Section 7 of SNC-3693-1. The test conditions were:

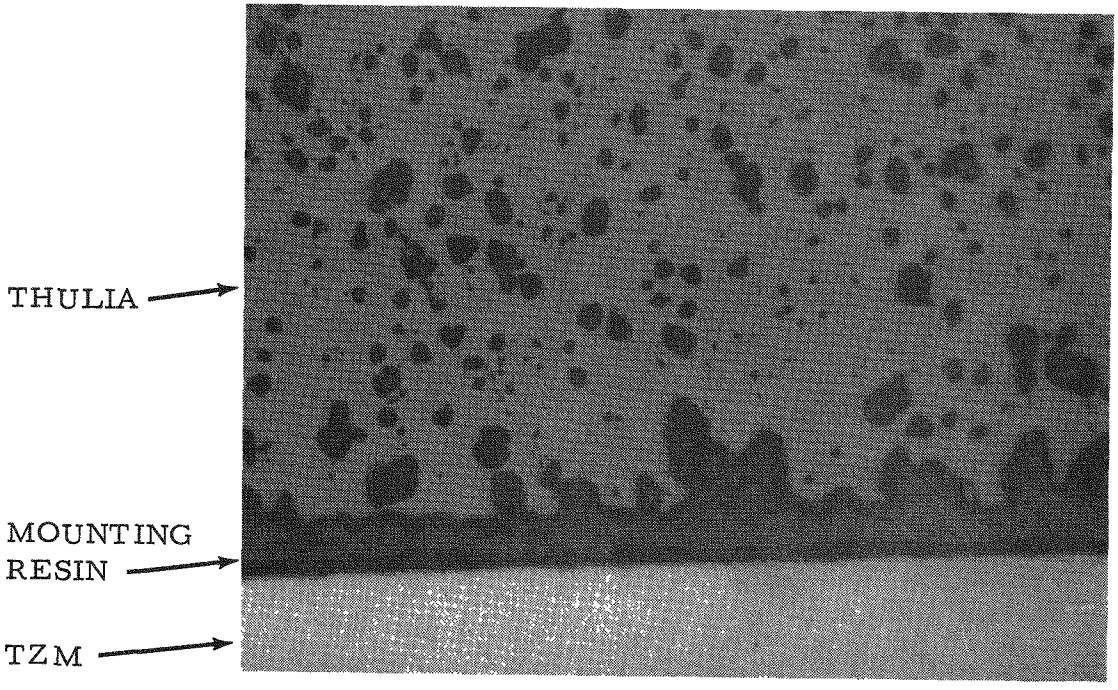

a. 90% Tm_2O_3 - 10% Yb_2O_3 wafer.
Note irregular surface.

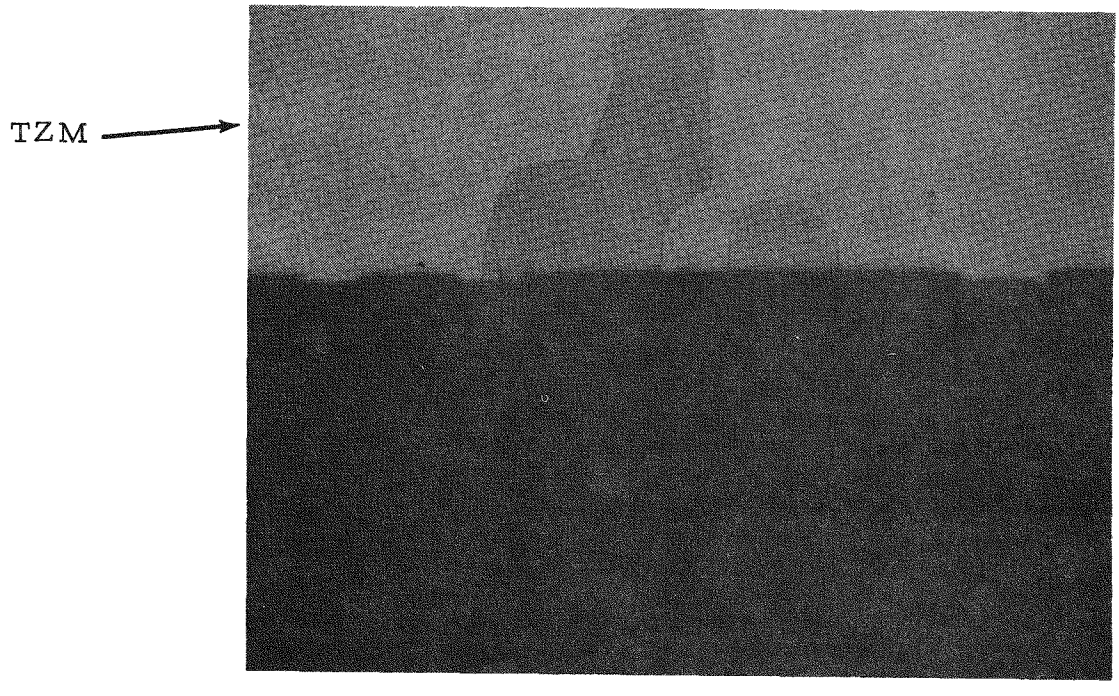

b. TZM

Figure 4-10. Micrographs of TZM/Thulia after 10,000 Hours at 1600°C. 100 X.

Tm_2O_3 composition:	Tm_2O_3 with 0, 5, 10 and 20% Yb_2O_3.
Time at temperature:	at 1600°C - 500, 2500 and 4000 hours ; at 2000°C - 500 hours.
Atmosphere:	static vacuum (sealed capsules)

The results of the evaluation are summarized as follows:

1. There was no detectable reaction visually or microscopically between the tungsten and Tm_2O_3, after 4000 hours at 1600°C and 500 hours at 2000°C.

2. No bonding occurred between the tungsten and Tm_2O_3 after 4000 hours at 1600°C. However, after 500 hours at 2000°C, Tm_2O_3 had vapor deposited on the tungsten surfaces. The degree of Tm_2O_3/tungsten reaction was limited to surface bonding.

3. After both the 4000 hour tests at 1600°C and 500 hour at 2000°C, there was no infusion of tungsten into the Tm_2O_3 nor Tm or Yb into the tungsten.

4. The structural and mechanical integrity of the Tm_2O_3 was maintained through all test cycles. The one exception was 100% Tm_2O_3 prepared by the SNC process that underwent a crystal modification after 500 hours at 2000°C. The resulting structure was not identified.

5. Addition of 5, 10 and 20% Yb_2O_3 to Tm_2O_3 had no observable effect on the compatibility of the tungsten - Tm_2O_3 system.

4.6.2 EVALUATION OF THE 10,000-HOUR TESTS

The 10,000-hour tests at 1600°C showed a difference in behavior between Tm_2O_3 prepared by the SRL and SNC processes. Tm_2O_3 prepared by the SRL process had not bonded with the tungsten and showed no evidence of interaction (Figures 4-11 and 4-12). Electron microprobe analysis detected no infusion of W into the thulia nor Tm or Yb into the tungsten. The crystalline structure was that of Tm_2O_3 as determined by X-ray diffraction analysis.

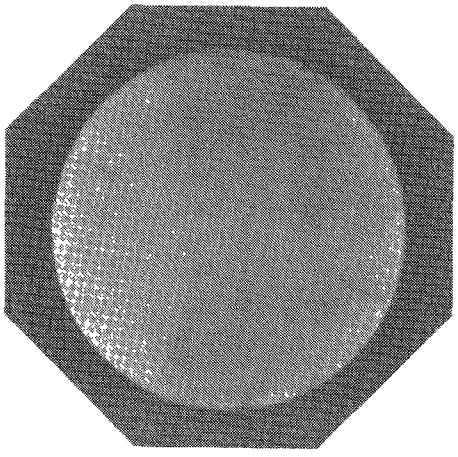

a. 100% Tm_2O_3

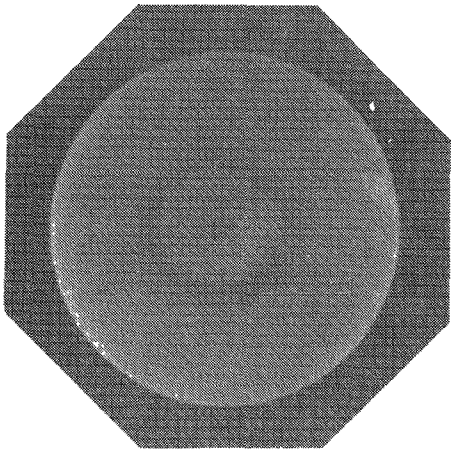

b. 90% Tm_2O_3 - 10% Yb_2O_3

Figure 4-11. Thulia Tested 10,000 Hours at 1600°C with Tungsten. Thulia Prepared by SRL Process.

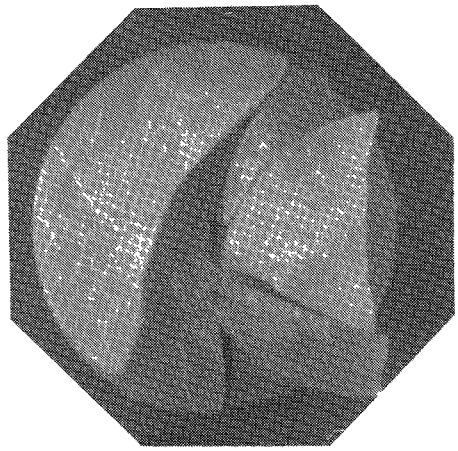

a. 100% Tm_2O_3

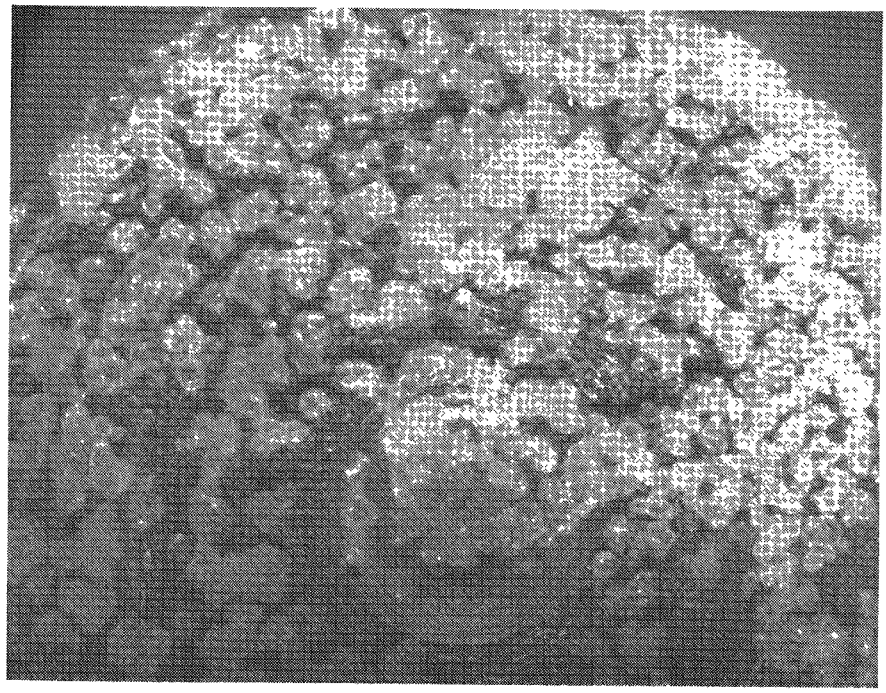

b. Vapor Deposited Crystals on Tungsten Capsule

Figure 4-12. Thulia Tested 10,000 Hours at 1600°C with Tungsten. Thulia Prepared by SNC Process.

The oxide wafers were mechanically sound and contained only minor radial cracks as were observed after the shorter term tests.

The Tm_2O_3 prepared by the SNC process exhibited different behavior in that some of the thulia transported to the tungsten capsule and that the crystalline structure of the remaining thulia was not that of Tm_2O_3. The surface of the thulia wafer had a glassy appearance unlike the companion samples prepared by the SRL process. X-ray diffraction analysis of the SNC process thulia showed no evidence of the Tm_2O_3 crystalline structure but rather a weak pattern of some unidentified compound.

Thulia tested in tungsten did not have the coarse crystalline texture as did the thulia tested in TZM. These results indicate that the behavior of thulia at 1600°C and above is influenced by trace amounts of other materials whether they be from the capsule material or residual impurities of the thulia.

With respect to the tungsten side of the compatibility couple, neither the SRL nor SNC process thulia reacted or infused in the tungsten (Figure 4-13). Likewise, thulia containing to 20% Yb_2O_3 showed no evidence of reaction with tungsten.

4.6.3 ASSESSMENT OF TUNGSTEN - Tm_2O_3 COMPATIBILITY

Tests at 1600°C for times to 10,000 hours and at 2000°C for 500 hours have shown that tungsten is resistant to any attack or penetration by Tm_2O_3 containing to 20% Yb_2O_3. However, the behavior of Tm_2O_3 in tungsten depended on the thulia processing prior to testing. Thulia prepared by the SRL process was essentially unaffected by the various tests with tungsten save for some changes in color; and therefore, was considered compatible. In contrast, thulia prepared by the SNC process exhibited sensitivity to tungsten in the form of enhanced vapor transport and the thulia changed to some unknown crystal form. Apparently, the combined effect of residual impurities in the thulia and the effect of tungsten were required to effect these changes since similar changes were not observed for SNC process thulia when tested in TZM. In fact, the SRL process material also showed vapor phase

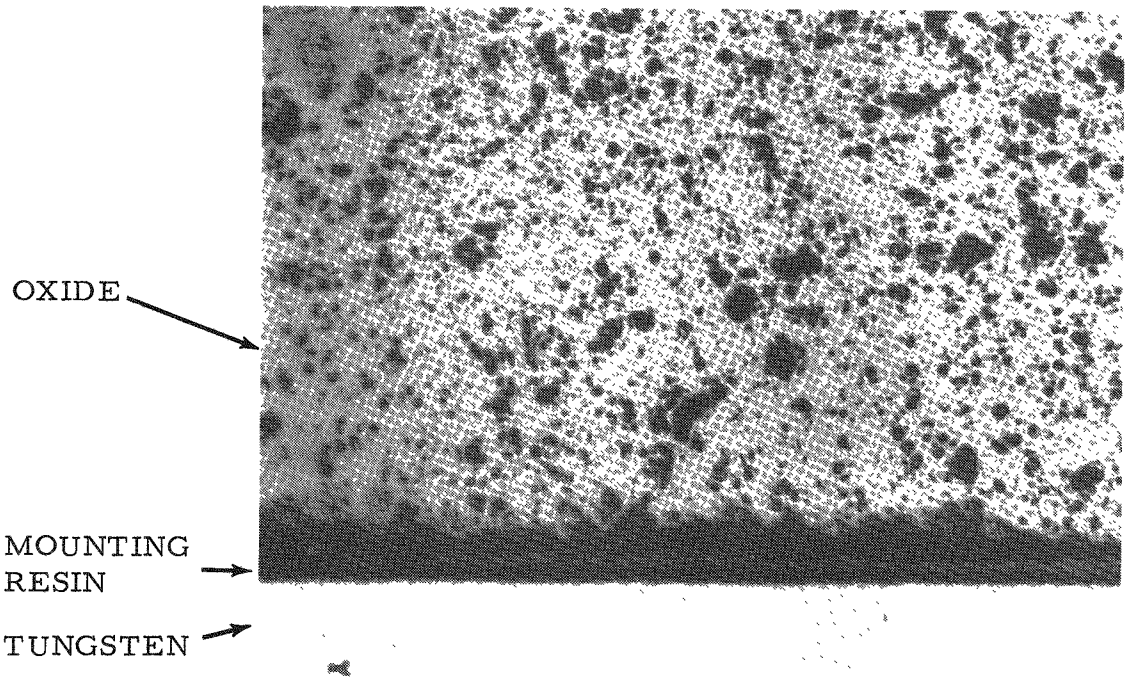

a. 90% Tm_2O_3 - 10% Yb_2O_3 Wafer

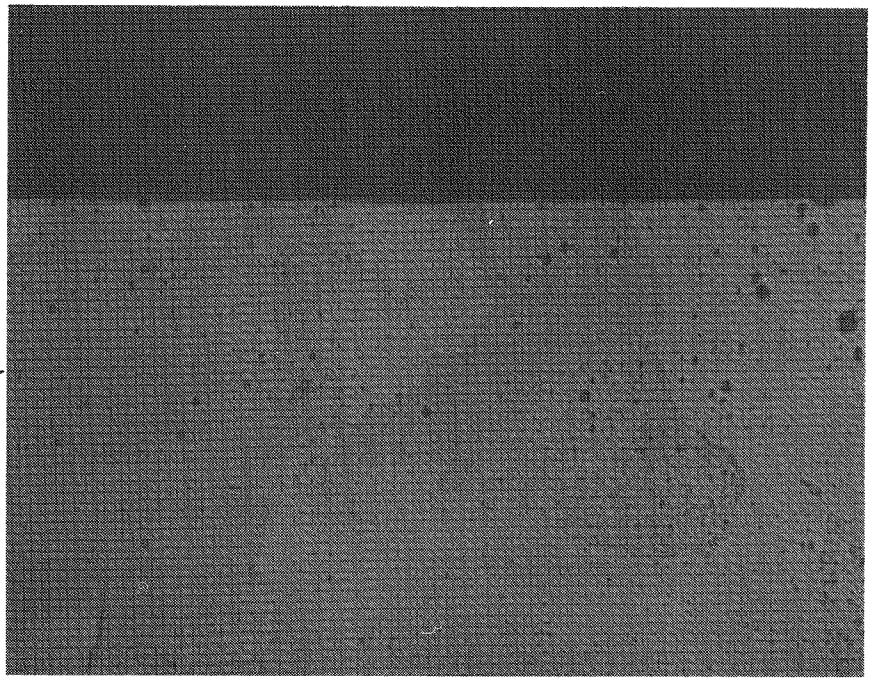

b. Tungsten

Figure 4-13. Micrographs of Tungsten/Thulia after 10,000 Hours at 1600°C. 100 X.

transport with TZM when tested at 1600°C. It can only be concluded that the behavior of thulia at 1600°C and above is effected by small amounts of other elements, possibly in combination. Such active elements have not yet been defined.

4.7 COMPATIBILITY OF ZIRCONIUM - Tm_2O_3/Yb_2O_3

4.7.1 SUMMARY OF PRIOR TESTS

No prior testing was performed of the zirconium - Tm_2O_3/ Yb_2O_3 system.

4.7.2 EVALUATION OF TESTS TO 6,500 HOURS

Compatibility tests were performed with zirconium under the following conditions:

Tm_2O_3 composition:	Tm_2O_3 with 0 and 20% Yb_2O_3
Times at temperature:	at 600°C - 500, 2500, 4000 and 6500 hours.
	at 1000°C - 500, 2500, 4000 and 6500 hours.
Atmosphere:	static vacuum (sealed capsules)

After testing to 6500 hours at 600°C, visual and microscopic examination showed no evidence of bonding or interaction between the zirconium and Tm_2O_3 (Figures 4-14 and 4-15). The oxide wafers were grey/green in color and contained minor radial cracks. The crystalline structure was that of Tm_2O_3 after 6500 hours at 600°C. Zirconium was not detected within the Tm_2O_3 but small amounts of Tm were found in localized areas within the Zr after 6500 hours.

Evaluation of tests at 1000°C showed evidence of interaction in the form of bonding and interdiffusion. After only 500 hours at 1000°C, the Tm_2O_3 had bonded to the zirconium and the thulia was colored a dark grey. After 2500 hours, electron microprobe analysis detected Tm penetration to a depth of at least 0.02 inch. Similar analysis showed no infusion of Zr into the thulia. After 6500 hours, x-ray diffraction analysis identified Tm_2O_3 plus some

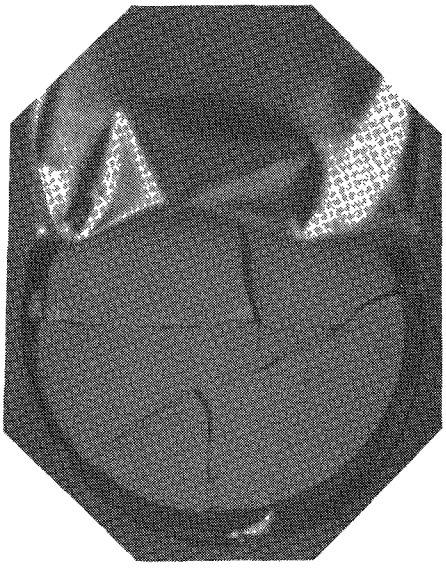

a. 100% Tm_2O_3 (SRL). Note Zr Foil Container About Tm_2O_3 Capsule

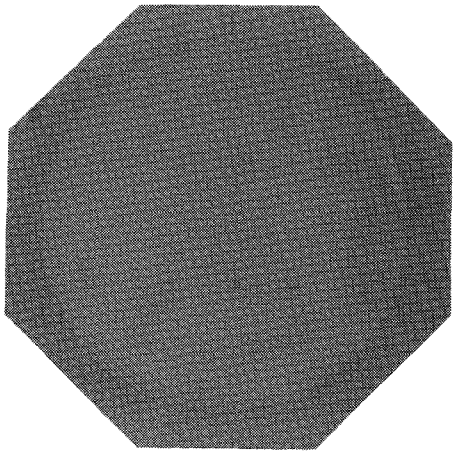

b. 80% Tm_2O_3 - 20% Yb_2O_3 (SRL)

Figure 4-14. Thulia Tested 6500 Hours at 600°C with Zirconium

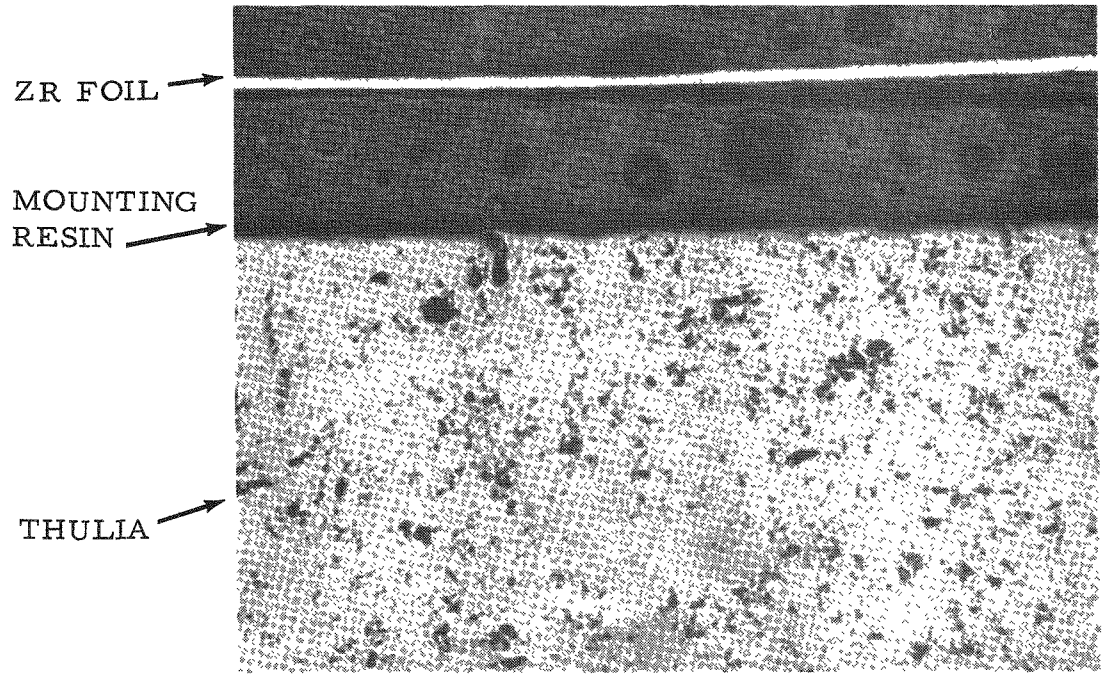

a. 100% Tm_2O_3 (SRL)

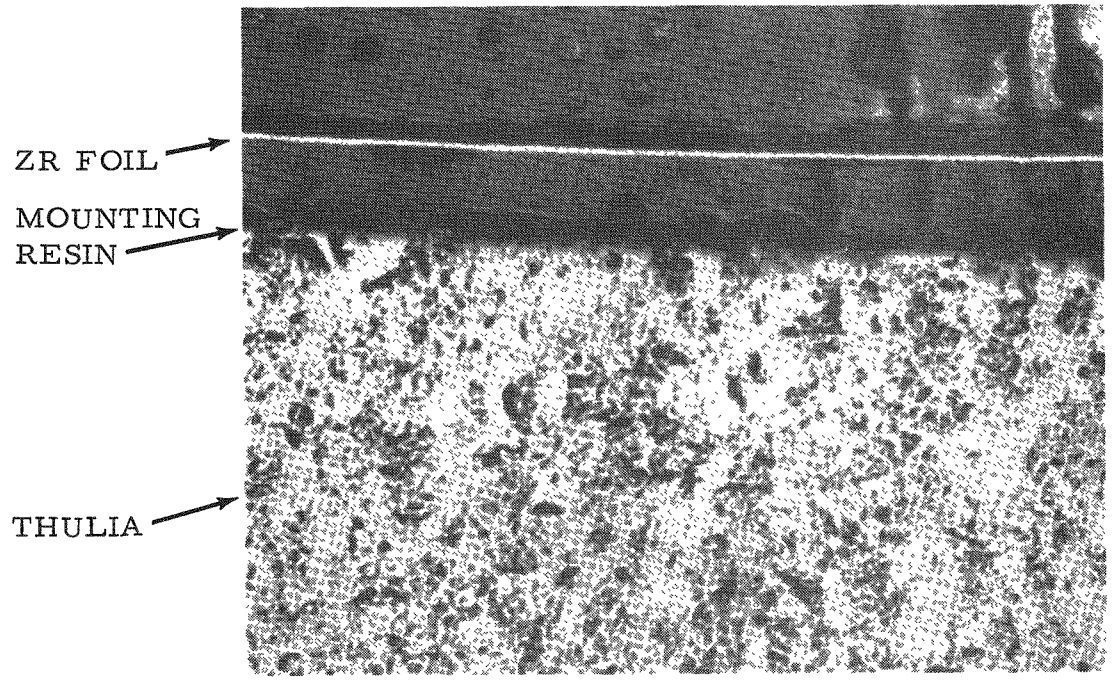

b. 80% Tm_2O_3 - 20% Yb_2O_3 (SRL)

Figure 4-15. Micrographs of Thulia Tested with Zirconium, 6500 Hours at 600°C. 100 X.

unidentified phase(s). The thulia wafers were severly cracked after all tests, the cause of the cracking was probably related to the partial collapse of the zirconium capsule at temperature (Figure 4-16). The capsules had "oil canned" at 1000°C due to the differential atmospheric pressure (the capsules were sealed under vacuum). None of the samples showed evidence of melting or reaction when examined microscopically (Figure 4-17). The addition of 20% Yb_2O_3 to the Tm_2O_3 had no detectable effect on the compatibility of the zirconium - Tm_2O_3 system at either 600 or 1000°C.

4.7.3 ASSESSMENT OF ZIRCONIUM - Tm_2O_3 COMPATIBILITY

The zirconium - Tm_2O_3 system was found to be compatible for at least 6500 hours at 600°C. Neither material showed evidence of interaction except for a color change in the Tm_2O_3. Also, the addition of 20% Yb_2O_3 to the Tm_2O_3 had no effect on the compatibility of the zirconium - Tm_2O_3 system.

At 1000°C, interaction between the zirconium and thulia was evidenced by bonding of the two materials, penetration of Tm into the zirconium, and by changes in the crystalline structure of the thulia. The mechanism by which the two materials interact is not known. Although the rates of interaction were not determined, it can be reasonably assumed that the interactions were continuous during the 1000°C tests. The degree of interaction of thulia with zirconium at 1000°C was greater than observed for Hastelloy-X, Haynes-25, T-111 and Hastelloy C-276. Notwithstanding its lesser compatibility, zirconium may still be considered as a container material if allowances be made for Tm interaction. It is doubtful that any interaction at 1000°C or less would lead to sudden or unexpected failure and, with care, the special properties of zirconium could well be utilized.

4.8 COMPATIBILITY OF HASTELLOY C-276 - Tm_2O_3/Yb_2O_3

4.8.1 SUMMARY OF PRIOR TESTS

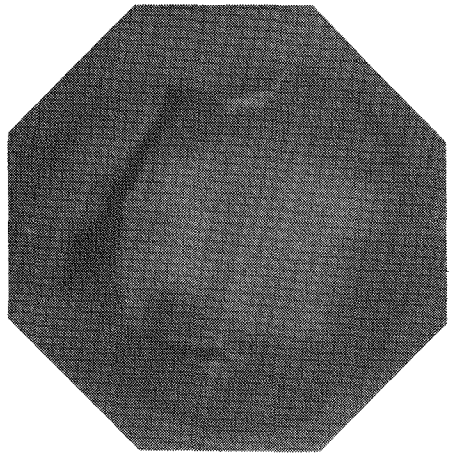

a. 100% Tm_2O_3 (SRL)

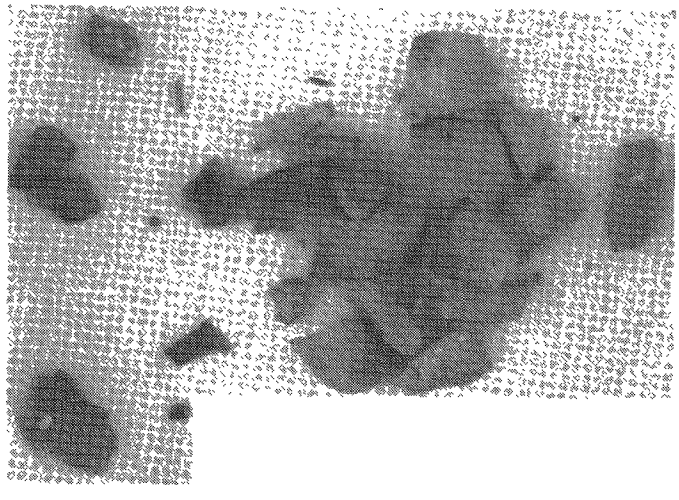

b. 80% Tm_2O_3 - 20% Yb_2O_3 (SRL)

Figure 4-16. Thulia Tested 6500 Hours at 1000°C with Zirconium

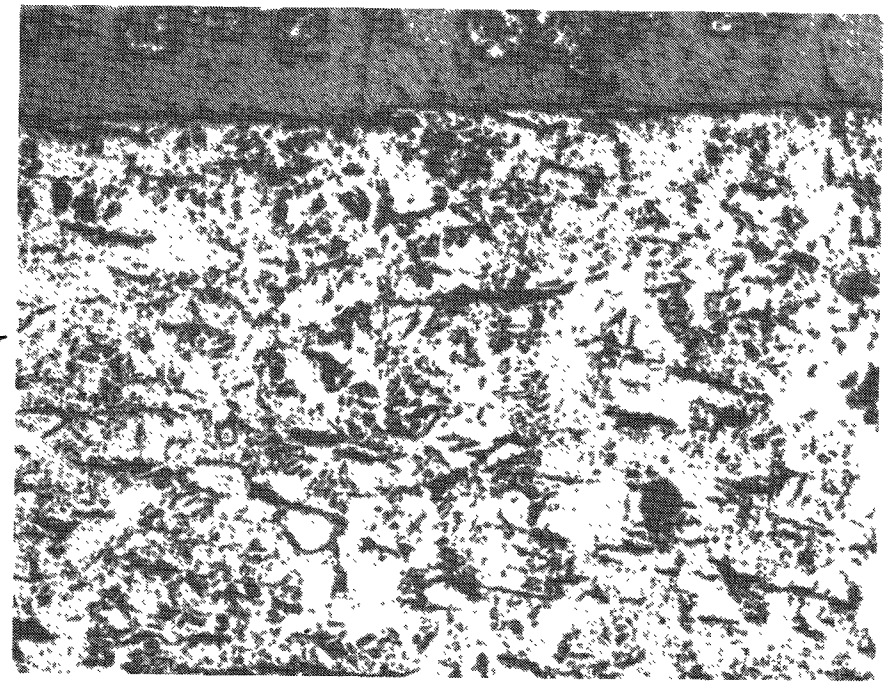

a. 100% Tm_2O_3 Wafer

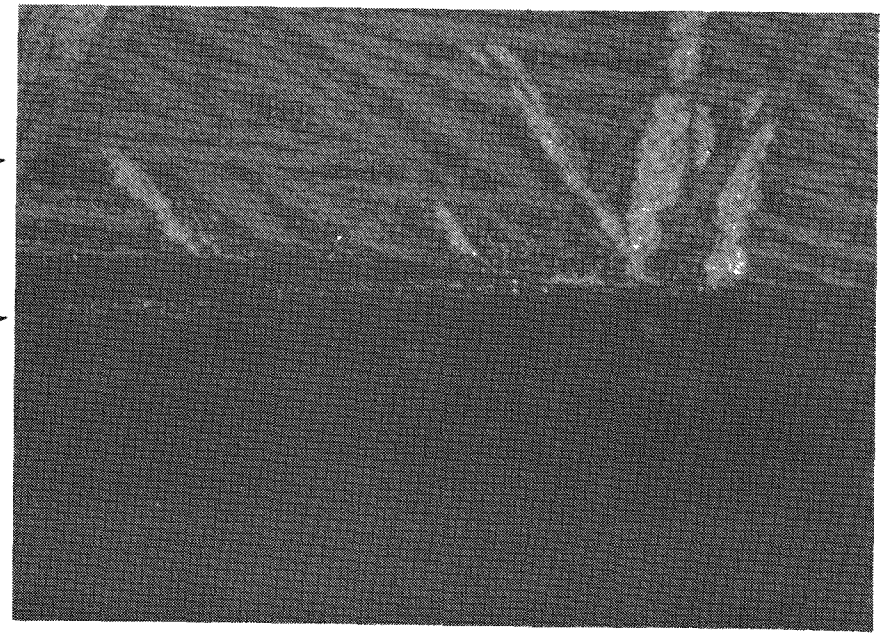

b. Zirconium

Figure 4-17. Micrographs of Thulia Tested with Zirconium, 2500 Hours at 1000°C. 100 X.

No prior testing was performed on the Hastelloy C-276 - Tm_2O_3 system.

4.8.2 EVALUATION OF TESTS TO 6500 HOURS

Compatibility tests were performed with Hastelloy C-276 under the following conditions:

Tm_2O_3 composition:	Tm_2O_3 with 0 and 20% Yb_2O_3
Time at temperatures:	at 600°C - 500, 2500, 4000 and 6500 hours.
	at 1000°C - 500, 2500, 4000 and 6500 hours.
Atmosphere:	static vacuum (sealed capsules).

Visual and microscopic examination of specimens tested to 6500 hours at both 600 and 1000°C showed no evidence of bonding or attack (Figures 4-18 through 4-20). The Tm_2O_3 wafers were discolored to a grey/green and contained only a few radial cracks. There was no evidence of powdering or mass transport of the oxide. The addition of 20% Yb_2O_3 to the thulia had no effect on the compatibility of the couples. The Tm_2O_3 crystalline structure was stable during all tests as determined by x-ray diffraction; there was no evidence of new phases. Although there was no visible evidence of interaction, electron microprobe analysis showed that small amounts of Cr and Co had deposited at the surface of the thulia after 4000 hours at both 600 and 1000°C. After 6500 hours at 1000°C, a small amount of Mo was found at the oxide surface, and Cr and Ni had penetrated the oxide wafer.

	6500 hours/1000°C	
	Cr	Ni
Oxide surface	0.5%	0.4%
10 microns below surface	0.1%	0.2%
30 microns below surface	0.05%	0.06%

The infusion of the alloy components of the Hastelloy C-276 apparently caused no changes in the Tm_2O_3 structure. Microprobe

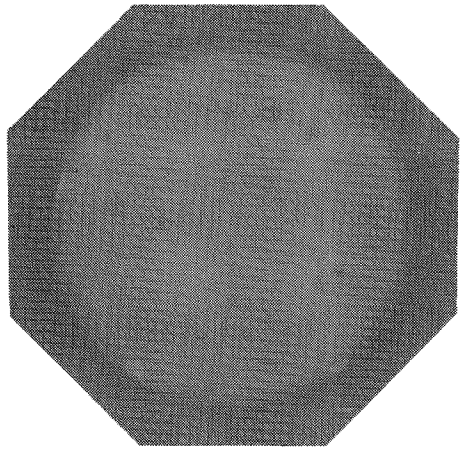

a. 100% Tm_2O_3 (SRL)

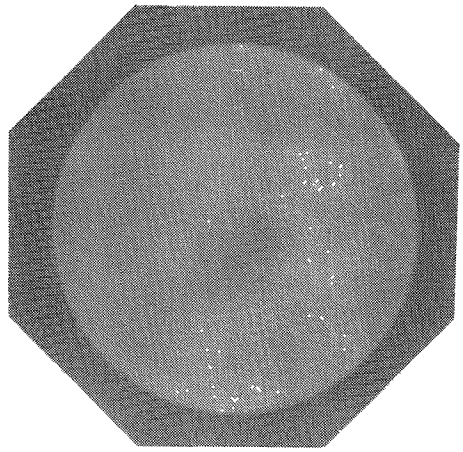

b. 80% Tm_2O_3 - 20% Yb_2O_3 (SRL)

Figure 4-18. Thulia Tested with Hastelloy C-276, 6500 Hours at 600°C.

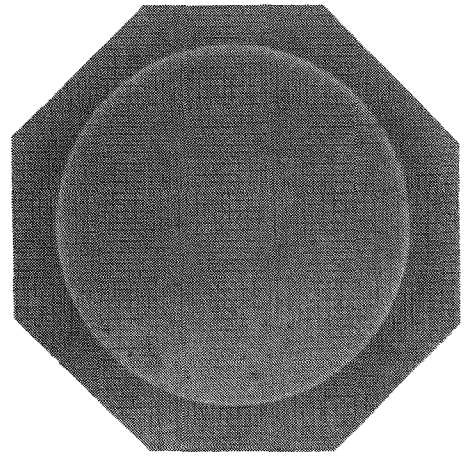

a. 100% Tm_2O_3 (SRL)

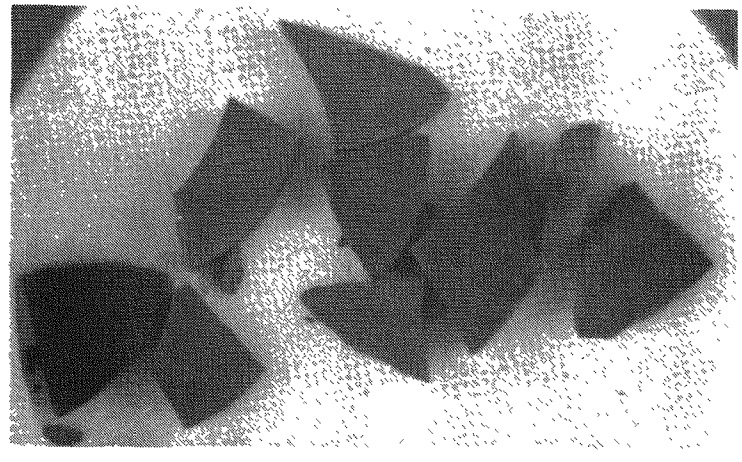

b. 80% Tm_2O_3 - 20% Yb_2O_3 (SRL)

Figure 4-19. Thulia Tested with Hastelloy C-276, 6500 Hours at 1000°C

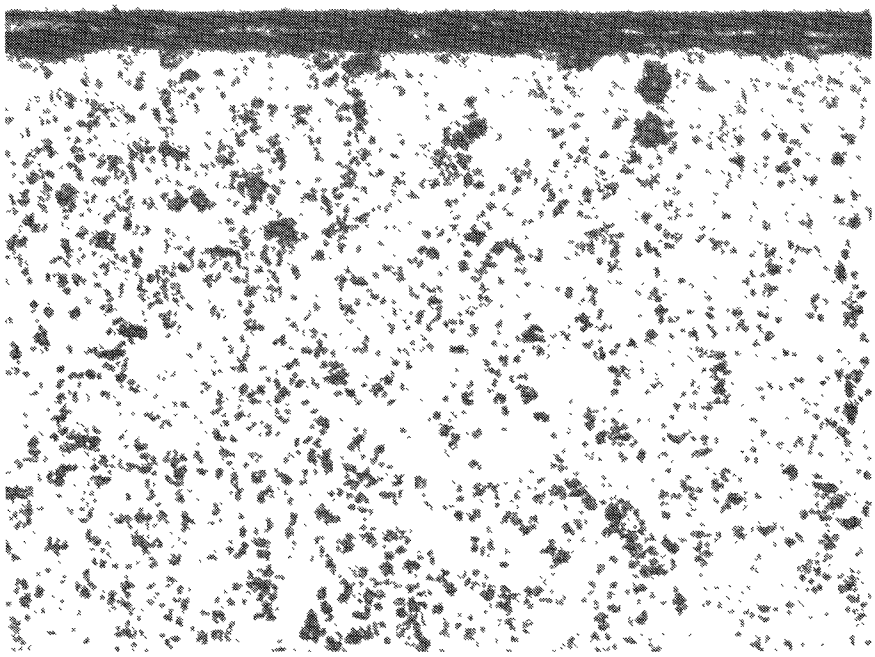

a. 100% Tm_2O_3 Wafer

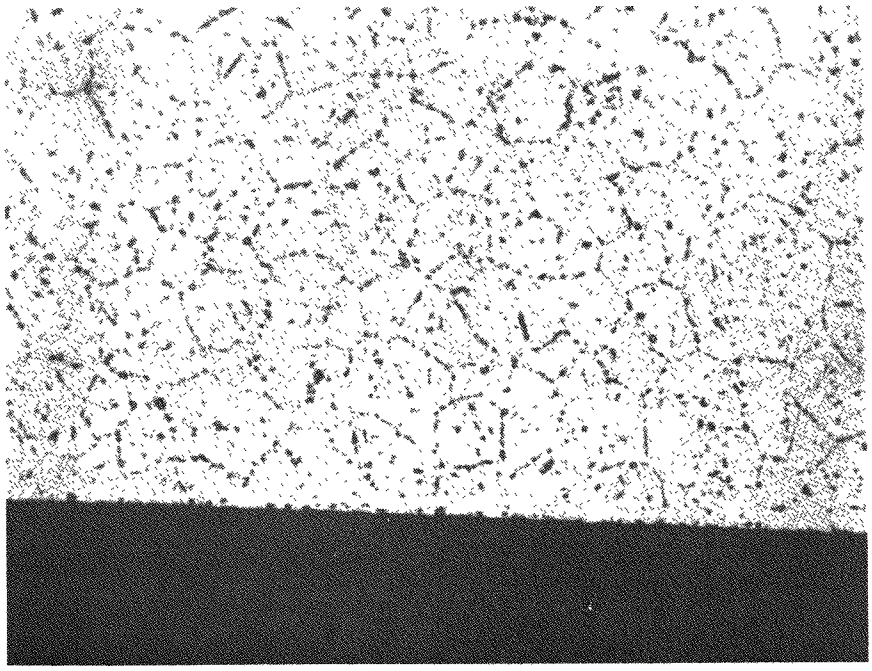

b. Hastelloy C-276

Figure 4-20. Micrographs of Hastelloy C-276/Thulia Tested 6500 Hours at 1000°C. 100 X.

analysis detected no infusion of Tm or Yb into the metal.

4.8.3 ASSESSMENT OF THE COMPATIBILITY OF HASTELLOY C-276 WITH Tm_2O_3

The tests at 600 and 1000°C for times to 6500 hours have shown that Hastelloy C-276 is unaffected by Tm_2O_3 with or without 20% Yb_2O_3. As indicated by the pick-up in the thulia, the metal lost small quantities of its various components such as Cr, Ni, and Mo. It is expected that these elements were transported by a simple vaporization mechanism and it is doubtful that either the Tm_2O_3 or the Yb_2O_3 had any effect but to serve as an accepter. The thulia maintained its structural and mechanical integrity during the various tests and showed no detrimental effects of the infusion of Cr and Ni. Thus, it can be concluded that Hastelloy C-276 is compatible with Tm_2O_3 at temperatures to at least 1000°C.

4.9 CONCLUSIONS

4.9.1 EVALUATION SUMMARY

The compatibility of Tm_2O_3 and Tm_2O_3/Yb_2O_3 containing up to 20% Yb_2O_3 was determined with seven candidate encapsulant materials. Determination of compatibility was based on the following:

- Penetration of Tm_2O_3/Yb_2O_3 into the encapsulant material
- Penetration of the encapsulant material into the Tm_2O_3/Yb_2O_3
- Structural changes in the thulia
- Physical changes in the thulia

Evaluations were performed by visual and metallographic examination, x-ray diffraction, x-ray fluorescence and electron microprobe analyses. A summary of the evaluations is given in Table 4-1. (The Yb_2O_3 content of the thulia showed no significant effect with respect to compatibility with the container materials, hence the Yb_2O_3 content is not shown as a variable.) The instrumental analyses were performed at a qualitative level to identify major effects; more detailed analyses were beyond the scope of this study.

TABLE 4-1

EVALUATION SUMMARY

Encapsulant Material	Penetration of Metal by Tm/Yb	Penetration of Tm_2O_3 by Metal	Structural Changes of Tm_2O_3	Physical Changes of Tm_2O_3
Hastelloy-X				
to 10,000 hrs-600°C	None detected*	None detected	Cracking and powdering	Slight coloration
10,000 hrs-1000°C	None detected	Trace Fe, Cr	Cracking and powdering	Slight coloration
Haynes 25				
to 10,000 hrs-600°C	None detected	Trace Cr, Co	Slight cracking & powdering	Slight coloration
10,000 hrs-1000°C	None detected	Trace Cr, Co	Slight cracking & powdering	Slight coloration
T-111				
to 10,000 hrs-1000°C	None detected	None detected	Cracking and powdering	Slight coloration
10,000 hrs-1600°C	None detected	0.004" reaction layer	Severe cracking and modification of crystalline structure	Deep coloration
TZM				
to 10,000 hrs-1600°C	None detected	None detected	None	Deep coloration (yellow & brown)
500 hrs-2000°C	None detected	Trace Ti	Slight cracking	Deep coloration (yellow)
Tungsten				
to 10,000 hrs-1600°C	None detected	None detected	Slight cracking	Moderate coloration (green)
500 hrs-2000°C	None detected	Trace W	Slight cracking & modification of crystalline structure	Moderate coloration (green)
Zirconium				
to 6500 hrs-600°C	Trace-localized	None detected	Cracking	Slight coloration
6500 hrs-1000°C	None detected	None detected	Severe cracking	Deep coloration (gray)
Hastelloy C-276				
to 6500 hrs-600°C	None detected	Trace Cr, Co	Slight cracking	Moderate coloration (grey/green)
6500 hrs-1000°C	None detected	Trace Cr, Ni, Mo	Slight cracking	Moderate coloration (grey/green)

*less than 3-micron penetration

Comparison of the compatibility of thulia prepared by two processes showed no difference in compatibility with respect to the encapsulant material. However, the behavior of the thulia was different for the two processes as indicated by the tendency toward translucence and toward modification in its crystalline structure after tests at 1600 and 2000°C. The difference in behavior was believed to be due, at least in part, to the impurity content of the thulia.

Based on the test data obtained from this study, it was concluded that Tm_2O_3/Yb_2O_3 can be successfully contained under the following conditions:

Container Material	Time, Hours	Maximum Temperature, °C
Hastelloy-X	10,000	1000
Haynes-25	10,000	1000
T-111	10,000	1600
TZM	10,000	1600
	500	2000
Tungsten	10,000	1600
	500	2000
Zirconium	6500	600
	Conditional Application over 500 hours	1000
C-276	6500	1000

The above encapsulant conditions are conservative since at these conditions no penetration of the encapsulant material was observed. Selection of specific encapsulant materials would be determined by system design and mission requirements. The demonstrated compatibility of the seven encapsulant materials with thulia provides considerable latitude to the system designer in encapsulant selection.

Although the Tm_2O_3/Yb_2O_3 did not enter the container materials during the various test cycles, some changes in the Tm_2O_3/Yb_2O_3 were observed. The mechanisms causing these changes were not known and their study was beyond the scope of this program. Observed changes in the oxide discs were:

- Slight powdering of the oxide after testin in Hastelloy-X at 600 and 1000°C and in T-111 at 1000°C.
- Increase in coloration of the oxide with increasing severity of tests.
- Change in crystalline structure of Tm_2O_3 (SNC Process) after testing with tungsten at 1600 and 2000°C, and Tm_2O_3 (SRL Process) with zirconium at 1000°C.
- Increase in degree of transparency to visible light with increasing severity of heat treatment of Tm_2O_3 tested in Haynes-25, Hastelloy X, and tungsten.
- Decrease in degree of transparency to visible light with increasing severity of heat treatment for Tm_2O_3 tested in T-111, TZM, zirconium, and Hastelloy C-276.

Although these changes were observed in the Tm_2O_3, they do not pose restriction of the application of Tm_2O_3 as a heat source except possibly in those applications where mechanical stability of the fuel is specified.

4.9.2 TABULATION

Tables 4-2 through 4-4 provide a tabulation of x-ray diffraction patterns of thulia wafers showing other than single phase Tm_2O_3. All data is reported as d-spacings as determined using diffractometer traces and nickel-filtered copper radiation. The abbreviations used are as follows:

vw = very weak
mw = medium weak
w = weak
m = medium
ms = medium strong
s = strong
vs = very strong
vvs = very, very strong

Tables 4-5 through 4-7 provide a compilation of test performed.

TABLE 4-2

X-RAY DIFFRACTION DATA
As Sintered (Blanks)
100% Tm_2O_3

SRL Process	SNC Process
4.31m	4.30m
3.04vs	3.04vs
2.81m	2.81w
2.63vs	2.63vs
2.48m	2.48m
2.35m	2.35w
2.24m	2.24m
2.14w	2.14w
2.06m	2.06m
1.92m	1.92w
1.86vs	1.86vs
1.80m	1.80w
	1.75w
1.71m	1.71m
1.66m	1.66w
1.62m	1.62m
1.58s	1.58s
1.55m	1.55m
1.51m	1.51m
1.48w	1.49w
1.46w	1.46w
1.43m	1.43w
1.44w	1.33w
1.31w	1.31w
1.29w	1.29w
1.27w	1.27w
1.25w	1.26w
1.24w	
1.22w	1.22w
1.20m	1.20m
1.17m	1.17m
1.15w	
1.13w	1.13w
1.11w	1.11w
1.08w	1.08w
1.07w	1.07w

TABLE 4-3

X-RAY DIFFRACTION DATA
SRL PROCESS WAFERS TESTED WITH ZIRCONIUM

Tested with Zirconium

100% Tm_2O_3 SRL Process 6500 hours at 1000°C	Tm_2O_3/20% Yb_2O_3 SRL Process 6500 hours at 1000°C
4.21m	3.02s
3.06m	2.71w
2.98s	2.60m
2.76w	2.55m
2.60s	2.45w
2.44w	2.04m
2.32w	1.90w
2.21w	1.85s
2.04w	1.79w
1.84s	1.69w
1.69m	1.57s
1.65w	1.56m
1.61w	1.20m
1.59w	1.17m
1.57s	
1.54m	
1.51m	
1.47w	
1.44w	
1.42w	

TABLE 4-4

X-RAY DIFFRACTION DATA

Tested with Tungsten 10,000 hours at 1600°C 100% Thulia, SNC Process	Tested with T-111 10,000 hours at 1600°C 90% Tm_2O_3/10% Yb_2O_3, SRL Process
3.59w	5.34w
1.79m	3.66w
1.29m	3.12s
1.25s	2.88s
1.20s	2.70s
1.08s	2.59s
0.96s	2.51m
0.89m	2.39m
0.88s	2.11w
0.80m	2.05w
	1.91m
	1.88s
	1.84s
	1.81w
	1.78w
	1.72w
	1.69m
	1.62m
	1.59m
	1.58m
	1.56m
	1.52m
	1.49m
	1.46m
	1.45s

TABLE 4-5

COMPILATION OF TESTS PERFORMED - HASTELLOY-X, HAYNES-25, T-111, TZM AND TUNGSTEN

Control Specimens	Specimens % Tm_2O_3/Yb_2O_3	Process	Macro Exam	Micro Exam	ANALYSES X-ray Diffraction	X-ray Fluorescence	Electron Microprobe	Cracking of Oxide	Bonding Oxide to Metal	Powdering of Oxide	Coloration of Oxide	Transparency
	Hastelloy X 600°C 10,000 hours											
	100/0	SRL	x	x	x			1	1	1	1	1
	95/5	SRL	x	x				2	1	1	1	1
x	95/5	SRL	x	x				1	1	1	1	1
	90/10	SRL	x	x			x	1	1	1	1	1
x	90/10	SRL	x	x				1	1	1	1	1
x	80/20	SRL	x	x	x			1	1	1	1	2
x	100/	SNC	x	x	x			1	1	1	1	1
	Hastelloy X 1000°C 10,000 hours											
	100/0	SRL	x	x	x			1	1	1	3	1
x	95/5	SRL	x	x				1	1	1	2	1
	95/5	SRL	x	x				2	1	1	3	1
	90/10	SRL	x	x				1	1	1	2	1
x	90/10	SRL	x	x			x	1	1	1	3	1
x	80/20	SRL	x	x	x			1	1	1	3	2
x	100/	SNC	x	x	x			1	1	2	1	3
	Haynes 25 600°C 10,000 hours											
	100/0	SRL	x	x				1	1	1	1	1
	95/5	SRL	x	x				1	1	1	1	1
	90/10	SRL	x	x	x		x	1	1	1	1	1
	Haynes 25 1000°C 10,000 hrs											
	100/0	SRL	x	x	x			3	1	1	2	2
	95/5	SRL	x	x				1	1	1	3	1
	90/10	SRL	x	x			x	1	1	1	3	1
	T-111 1000°C 10,000 hrs											
	100/0	SRL	x	x	x		x	1	1	1	1	1
	90/10	SRL	x	x	x		x	2	1	1	1	1
	T-111 1600°C 10,000 hrs											
	90/10	SRL	x	x	x		x	3	3	3	3	3
	TZM 1600°C 10,000 hrs											
	90/10	SRL	x	x	x		x	1	3	1	3	2
	Tungsten 1600°C 10,000 hrs											
x	100/0	SRL	x	x	x		x	1	1	1	1	2
	90/10	SRL	x	x	x			1	2	1	2	2
x	100/0	SNC	x	x	x			3	2	1	2	3

TABLE 4-6

COMPILATION OF TESTS - ZIRCONIUM

Specimens % Tm_2O_3/Yb_2O_3	Process	Macro exam	Micro exam	X-ray Diffraction		X-ray Fluorescence	Electron Micro Probe	Cracking of Oxide	Bonding of Metal	Powdering of Oxide	Coloration of Oxide		Transparency
Zirconium 600°C 500 hr													
100/0	SRL	X	X		*			1	3	1	2		1
80/20	SRL	X	X					1	3	1	2		1
Zirconium 600°C 2500 hr													
100/0	SRL	X	X					1	3	1	2		1
80/20	SRL	X	X					1	3	1	2		1
Zirconium 600°C 4000 hr													
100/0	SRL	X	X					1	3	1	3		1
80/20	SRL	X	X				X	1	3	1	2		2
Zirconium 600°C 6500 hr													
100/0	SRL	X	X	X			X	3	3	1	1		1
80/20	SRL	X	X	X			X	1	3	1	2		1
Zirconium 1000°C 500 hr													
100/0	SRL	X	X					3	3	1	3		1
80/20	SRL	X	X					3	3	1	3		1
Zirconium 1000°C 2500 hr													
100/0	SRL	X	X					3	3	1	3		1
80/20	SRL	X	X					3	3	1	3		1
Zirconium 1000°C 4000 hr													
100/0	SRL	X						*					
80/20	SRL	X						*					
Zirconium 1000°C 6500 hr													
100/0	SRL	X	X	X				3	3	1	3		1
80/20	SRL	X	X	X				3	3	1	2		1

* capsules oxidized during test - samples destroyed

TABLE 4-7

COMPILATION OF TESTS - HASTELLOY C-276

Specimens % Tm_2O_3/Yb_2O_3 Process	ANALYSES: Macro exam	Micro exam	X-ray Diffraction	X-ray Fluorescence	Electron Micro-Probe	Cracking of Oxide	Bonding of Metal	Powdering of Oxide	Coloration of Oxide	Transparency
Hastelloy C-276										
600°C 500 hrs										
100/0 SRL	x	x				1	1	1	2	1
80/20 SRL	x	x				1	1	1	2	2
Hastelloy C-276										
600°C 2500 hrs										
100/0 SRL	x	x				1	1	1	2	1
80/20 SRL	x	x				1	1	1	1	2
Hastelloy C-276										
600°C 4000 hrs										
100/0 SRL	x	x	x			1	1	1	1	2
80/20 SRL	x	x	x		x	1	1	1	1	1
Hastelloy C-276										
600°C 6500 hrs										
100/0 SRL	x	x	x			1	1	1	2	2
80/20 SRL	x	x	x			1	1	1	1	1
Hastelloy C-276										
1000°C 500 hrs										
100/0 SRL	x	x				1	1	1	3	1
80/20 SRL	x	x				1	1	1	3	2
Hastelloy C-276										
1000°C 2500 hrs										
100/0 SRL	x	x				1	1	1	2	2
80/20 SRL	x	x				1	1	1	3	2
Hastelloy C-276										
1000°C 4000 hrs										
100/0 SRL	x	x	x			1	1	1	2	2
80/20 SRL	x	x	x		x	2	1	1	2	1
Hastelloy C-276										
1000°C 6500 hrs										
100/0 SRL	x	x	x		x	1	1	1	2	2
80/20 SRL	x	x	x			3	1	1	3	1

SECTION 5
THULIUM-170 OXIDE HEAT SOURCE EXPERIMENTAL AND ANALYTICAL RADIATION AND SHIELDING STUDY

5.1 INTRODUCTION

Several materials have been identified as potential shielding materials for thulium oxide heat sources. A knowledge of their properties is essential before an assessment of feasibility of application of the oxide can be made. The discussion herein relates to the application of several types of shielding materials to a representative pressed, sintered and activated Tm_2O_3 source, and the development of techniques and methods of analysis that will allow calculated dose rates to predict reliably those dose rates to be experienced experimentally.

Dose rates from 5, 10 and 20.7-watt Tm_2O_3 sources at two different source-to-dose-point distances (19 and 100 cm) were experimentally determined using thermoluminescent dosimetry techniques. Five different absorber materials (aluminum, stainless steel, lead, tungsten and depleted uranium) of three different thicknesses (¼, ½ and 1") were used.

5.2 EXPERIMENTAL DOSE RATE DETERMINATIONS

The radiation dose rates from Tm-170 sources were determined by measurement of the luminescence of lithium fluouride phosphors in a Con-Rad Model 5100B Readout instrument. Each measurement utilized five separate TLD dosimeters to assure high reliability of the test results. Figure 5-1 shows the experimental configuration including a shielded enclosure for sources; holder for shielding

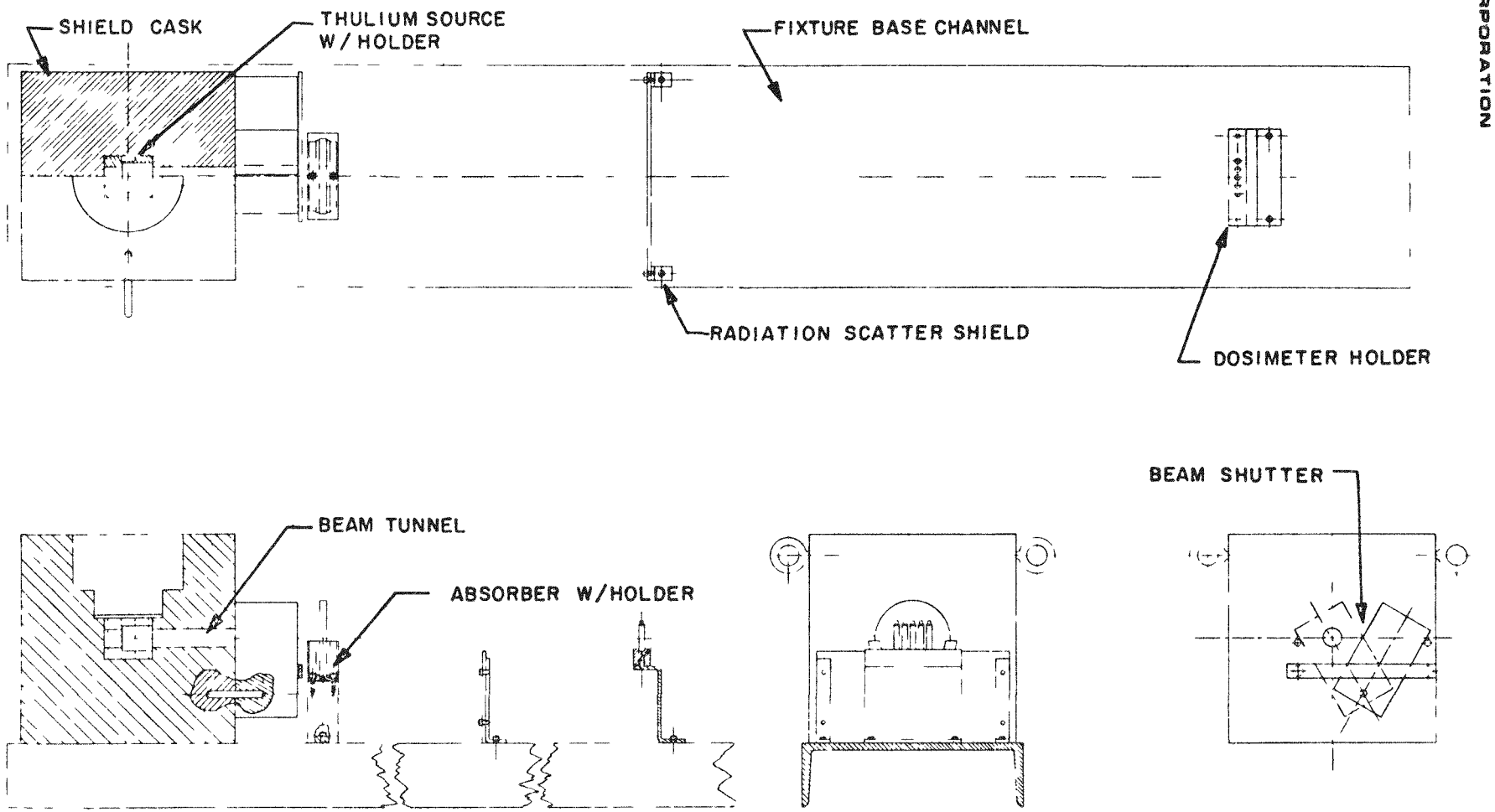

Figure 5-1. Thulium-170 Oxide Dosimeter Configuration

materials and TLD dosimeters.

Background doses were subtracted from the measured values. The net dose rates (rads/hr) were determined by dividing the net doses (rads) by the exposure time in hours. These dose rates were then normalized corresponding to the decay factor from initial activity. The overall uncertainty (experimental error) in the measured dose rate was ± 9%. The final experimental results are presented in Tables 5-1 through 5-5.

5.3 THEORETICAL DOSE RATE DETERMINATIONS

The basic equation used to calculate the uncollided radiation dose rate for monoenergetic gamma rays of initial energy E_o is [19][20]:

$$D_{uncollided}\ (E_o) = 5.767 \times 10^{-2}\ (\frac{\mu_\sigma}{\rho})_{tissue}\ E_o\ \phi\ (E_o)$$

For cylindrical source geometry and an axial dose point:

$$\phi\ (E_o) = \frac{S_v}{2\mu_s}\left[E_2\ (b_1) - E_2\ (b_3) + \frac{E_2\ (b_3 \sec\theta)}{\sec\theta} - \frac{E_2\ (b_1 \sec\theta)}{\sec\theta}\right]$$

The total dose rate then is given by:

$$D_{total}\ (E_o) = B_\infty\ (E_o)\ D_{uncollided}\ (E_o)$$

For a composite gamma spectrum with n groups of gamma rays of initial energies E_1, E_2 ..... E_n, the total dose rate for the entire spectrum is:

$$D_{total} = \sum_{i=1}^{n} D_{total}\ (E_i)$$

For Tm-170, although the decay scheme[21] (Figure 5-2) gives only a single energy gamma, the bremsstrahlung radiation produced by beta particles constitutes a continuous gamma spectrum with maximum energy of 0.968 Mev[19]. Table 5-6 gives the total electromagnetic radiation spectrum used in the calculation of

TABLE 5-1

DATA SUMMARY FOR ALUMINUM ABSORBERS

Initial Source Strength (watts)	Absorber Thickness (inches)	Exposure Time (hours)	Measured Dose (rads)	Net Dose (rads)	Net Dose Rate (rads/hr)	Measured* Dose Rate (rads/hr)	Calculated Dose Rate (rads/hr)	Ratio Calculated to Measured
1. 19 cm								
20.7	¼	0.25	21.7 ± .3	21.7	86.8	178 ± 2	161	0.90
	½	0.25	20.9 ± .2	20.9	83.6	171 ± 2	160	0.94
	1	0.25	16.2 ± .2	16.2	64.7	132 ± 2	156	1.18
10	¼	0.25	17.8 ± .3	17.8	71.0	141 ± 2	119	0.84
	½	0.25	14.3 ± .1	14.2	57.0	113 ± 1	118	1.04
	1	0.25	12.5 ± .1	12.4	49.7	98.5 ± .9	115	1.17
5	¼	0.25	11.7 ± .1	11.7	46.8	94.7 ± 1	81.6	0.86
	½	0.25	9.10 ± .03	9.06	36.2	73.2 ± .3	81.1	1.11
	1	0.25	6.50 ± .04	6.46	25.8	52.2 ± .3	79.0	1.51
2. 100 cm**								
20.7	¼	0.5	2.18 ± .01	2.05	4.10	3.70 ± .03	5.80	1.02
	½	0.5	1.86 ± .01	1.74	3.47	4.82 ± .02	5.80	1.20
	1	0.5	1.35 ± .01	1.23	2.46	3.42 ± .02	5.60	1.64
10	¼	0.5	1.22 ± .01	1.19	2.37	4.70 ± .03	4.30	0.92
	½	0.5	1.06 ± .01	1.03	2.05	4.06 ± .01	4.30	1.06
	1	0.5	.697 ± .003	.668	1.34	2.64 ± .01	4.20	1.59
5	¼	1	2.17 ± .01	2.05	2.05	2.58 ± .01	2.96	1.15
	½	1	1.81 ± .01	1.69	1.69	2.13 ± .01	2.92	1.37
	1	4	4.77 ± .02	4.65	1.16	1.47 ± .01	2.85	1.94

*Dose rate is normalized to correspond to the initial source strength.

**The calculated dose rates for source-to-dose point distance of 100 cm have been adjusted to reflect non-inverse square relationship.

TABLE 5-2

DATA SUMMARY FOR STAINLESS STEEL ABSORBERS

Initial Source Strength (watts)	Absorber Thickness (inches)	Exposure Time (hours)	Measured Dose (rads)	Net Dose (rads)	Net Dose Rate (rads/hr)	Measured* Dose Rate (rads/hr)	Calculated Dose Rate (rads/hr)	Ratio Calculated to Measured
1. 19 cm								
20.7	¼	.25	16.1 ± ..	16.1	64.2	131 ± 2	132	1.01
	½	.25	9.01 ± .05	8.99	36.0	73.6 ± .4	102	1.38
	1	.25	3.95 ± .03	3.94	15.7	32.2 ± .2	59	1.83
10	¼	.25	10.80 ± .05	10.7	43	87.6 ± .4	95.4	1.09
	½	.25	6.81 ± .05	6.80	27.2	55.4 ± .4	73.4	1.32
	1	.25	3.08 ± .04	3.07	12	24.4 ± .3	41.2	1.68
5	¼	.25	7.15 ± .05	7.11	28.4	57.2 ± .4	63.6	1.11
	½	.25	4.35 ± .04	4.32	17.3	34.6 ± .3	48.1	1.38
	1	.25	1.90 ± .02	1.86	7.45	15.0 ± .2	26.3	1.75
2. 100 cm **								
20.7	¼	.5	1.66 ± .01	1.53	3.06	4.20 ± .02	4.77	1.13
	½	.5	.996 ± .003	.869	1.74	2.36 ± .01	3.72	1.56
	1	.5	.460 ± .001	.333	.666	.911 ± .004	2.13	2.34
10	¼	.75	1.26 ± .01	1.24	1.65	3.25 ± .01	3.43	1.05
	½	.75	.717 ± .002	.689	.918	1.81 ± .01	2.64	1.46
	1	1.5	.492 ± .002	.464	.31	.610 ± .002	1.48	2.42
5	¼	1.5	2.01 ± .01	1.89	1.26	1.62 ± .01	2.30	1.42
	½	1.5	1.16 ± .01	1.04	.695	.862 ± .005	1.73	1.94
	1	1.5	.482 ± .003	.366	.244	.313 ± .002	0.94	3.00

*Dose rate is normalized to correspond to the initial source strength.

**The calculated dose rates for source-to-dose point distance of 100 cm have been adjusted to reflect non-inverse square relationship.

TABLE 5-3

DATA SUMMARY FOR LEAD ABSORBERS

Initial Source Strength (watts)	Absorber Thickness (inches)	Exposure Time (hours)	Measured Dose (rads)	Net Dose (rads)	Net Dose Rate (rads/hr)	Measured* Dose Rate (rads/hr)	Calculated Dose Rate (rads/hr)	Ratio Calculated to Measured
1. 19 cm								
20.7	¼	.25	3.09 ± .02	3.07	12.3	25.2 ± .2	27.3	1.08
	½	.25	.850 ± .003	.837	3.34	6.85 ± .02	8.72	1.27
	1	1.5	.751 ± .004	.738	.492	1.01 ± .01	1.32	1.31
10	¼	.25	1.96 ± .03	1.94	7.77	15.8 ± .2	17.2	1.09
	½	.5	1.23 ± .01	1.21	2.42	4.93 ± .03	5.27	1.07
	1	3	.973 ± .003	.958	.319	.650 ± .002	.774	1.19
5	¼	.25	1.24 ± .01	1.20	4.79	9.65 ± .11	9.97	1.03
	½	.5	.708 ± .003	.671	1.34	2.71 ± .01	2.98	1.1
	1	3.5	.735 ± .003	.698	.200	.402 ± .002	.43	1.07
2. 100 cm	**							
20.7	¼	1	.772 ± .003	.643	.643	.886 ± .004	.970	1.10
	½	2	.473 ± .001	.344	.172	.237 ± .001	.310	1.31
	1	15	.499 ± .002	.370	.0247	.0341 ± .0002	.047	1.38
10	¼	1	.486 ± .002	.37	.37	.493 ± .002	.614	1.24
	½	3	.420 ± .001	.304	.101	.135 ± .001	.190	1.41
	1	20	.376 ± .001	.26	.013	.0174 ± .0001	.026	1.61
5	¼	4	1.22 ± .01	1.07	.268	.348 ± .001	.360	1.04
	½	15	.959 ± .004	.814	.0542	.0705 ± .0003	.110	1.56
	1	74	.660 ± .004	.515	.00696	.00916 ± .00006	.0155	1.70

*Dose rate is normalized to correspond to the initial source strength.

**The calculated dose rates for source-to-dose point distance of 100 cm have been adjusted to reflect non-inverse square relationship.

TABLE 5-4

DATA SUMMARY FOR TUNGSTEN ABSORBERS

Initial Source Strength (watts)	Absorber Thickness (inches)	Exposure Time (hours)	Measured Dose (rads)	Net Dose (rads)	Net Dose Rate (rads/hr)	Measured* Dose Rate (rads/hr)	Calculated Dose Rate (rads/hr)	Ratio Calculated to Measured
1. 19 cm								
20.7	¼	.25	1.93 ± .02	1.90	7.61	14.9 ± .2	16.6	1.11
	½	.5	.802 ± .004	.78	1.56	3.06 ± .02	3.7	1.21
	1	6.25	.842 ± .005	.82	.131	.257 ± .002	.288	1.12
10	¼	.25	1.22 ± .01	1.18	4.73	9.22 ± .1	10.2	1.11
	½	.75	.755 ± .003	.721	.96	1.87 ± .01	2.21	1.18
	1	22.5	1.65 ± .02	1.62	.072	.139 ± .002	.167	1.19
5	¼	1	2.62 ± .03	2.6	2.6	5.04 ± .05	5.85	1.16
	½	2	1.10 ± .01	1.08	.539	1.05 ± .01	1.23	1.17
	1	18	.765 ± .006	.744	.0413	.0801 ± .0006	.092	1.15
2. 100 cm**								
20.7	¼	1.25	.380 ± .002	.311	.249	.433 ± .003	.600	1.38
	½	4.5	.274 ± .002	.205	.0456	.0793 ± .0006	.134	1.69
	1	72.5	.299 ± .002	.230	.00318	.00559 ± .00003	.010	1.79
10	¼	2	.362 ± .002	.303	.152	.256 ± .001	.370	1.45
	½	7	.257 ± .001	.198	.0283	.0478 ± .0002	.079	1.65
	1	120	.286 ± .001	.227	.0019	.00325 ± .00004	.006	1.85
5	¼	3	.419 ± .002	.268	.0893	.144 ± .001	.210	1.46
	½	18	.451 ± .005	.3	.0167	.0269 ± .0005	.044	1.63
	1	168	.350 ± .001	.199	.00118	.00194 ± .00002	.0033	1.70

*Dose rate is normalized to correspond to the initial source strength.

**The calculated dose rates for source-to-dose point distance of 100 cm have been adjusted to reflect non-inverse square relationship.

TABLE 5-5

DATA SUMMARY FOR DEPLETED URANIUM ABSORBERS

Initial Source Strength (watts)	Absorber Thickness (inches)	Exposure Time (hours)	Measured Dose (rads)	Net Dose (rads)	Net Dose Rate (rads/hr)	Measured*+ Dose Rate (rads/hr)	Calculated Dose Rate (rads/hr)	Ratio Calculated to Measured
1. 19 cm								
20.7	¼	1	3.12 ± .03	3.03	3.03	5.61 ± .06	7.71	1.37
	½	2	1.09 ± .01	1.01	.503	.888 ± .009	1.17	1.32
	1	48	3.84 ± .02	3.76	.0784	.0548 ± .001	.05	0.91
10	¼	1	1.96 ± .01	1.88	1.875	3.38 ± .02	4.65	1.37
	½	3	1.01 ± .01	.927	.309	.513 ± .005	.68	1.32
	1	88	5.97 ± .04	5.89	.067	.0318 ± .001	.029	0.91
5	¼	1	1.23 ± .02	1.15	1.15	1.98 ± .03	2.62	1.32
	½	4	.932 ± .004	.848	.212	.324 ± .002	.397	1.23
	1	108	6.98 ± .05	6.89	.0638	.0226 ± .001	.016	0.71
2. 100 cm	**							
20.7	¼	2	.422 ± .001	.282	.141	.218 ± .001	.280	1.28
	½	20	.511 ± .001	.371	.0185	.0286 ± .0001	.042	1.47
	1	169	.406 ± .001	.226	.00157	.0025 ± .00002	.0018	0.72
10	¼	3	.499 ± .002	.356	.119	.165 ± .001	.170	1.03
	½	24	.441 ± .002	.298	.0124	.0174 ± .0001	.025	1.44
	1	168	.345 ± .001	.202	.0012	.00172 ± .00001	.001	0.58
5	¼	6	.437 ± .001	.298	.05	.0733 ± .0002	.094	1.28
	½	65	.554 ± .001	.415	.00638	.00946 ± .00003	.014	1.48
	1	168	.241 ± .001	.102	.0006	.00091 ± .000006	.00053	0.64

*Dose rate is normalized to correspond to the initial source strength.

+Uranium background is subtracted.

**The calculated dose rates for source-to-dose point distance of 100 cm have been adjusted to reflect non-inverse square relationship.

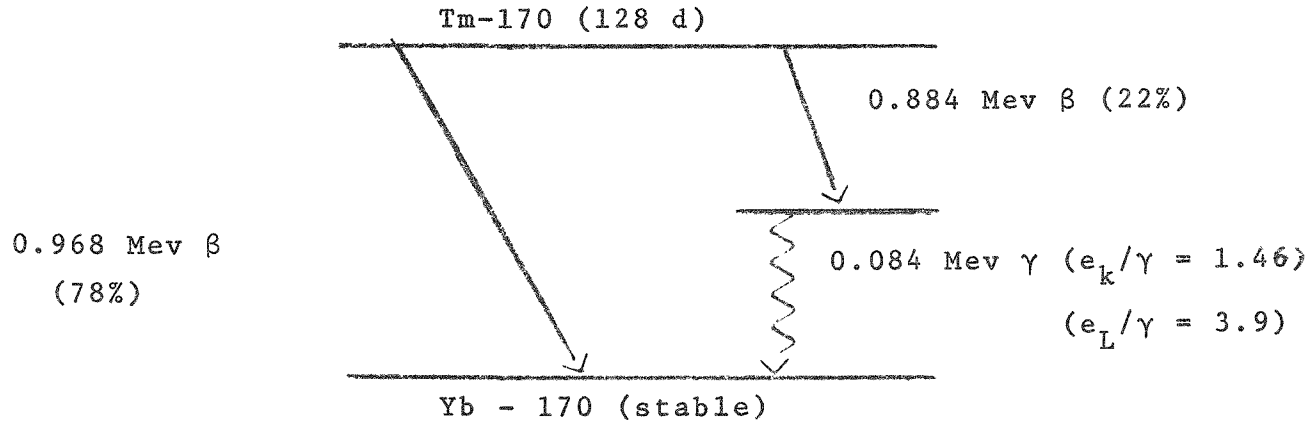

Figure 5-2 Decay Scheme of Tm-170

TABLE 5-6

GAMMA SPECTRUM OF Tm_2O_3 SOURCE*

Types of Radiation	Photon Energy (Mev)	Photons per Disintegration
Gamma	0.084	3.459×10^{-2}
X-ray	0.052	5.050×10^{-2}
X-ray	0.009	1.349×10^{-1}
Bremsstrahlung	0.05	5.574×10^{-2}
	0.1	2.014×10^{-2}
	0.015	9.857×10^{-3}
	0.2	5.430×10^{-3}
	0.25	3.169×10^{-3}
	0.3	1.903×10^{-3}
	0.35	1.155×10^{-3}
	0.4	6.992×10^{-4}
	0.45	4.180×10^{-4}
	0.5	2.441×10^{-4}
	0.55	1.377×10^{-4}
	0.6	7.386×10^{-5}
	0.65	3.700×10^{-5}
	0.7	1.683×10^{-5}
	0.75	6.669×10^{-6}
	0.8	2.136×10^{-6}
	0.85	4.778×10^{-7}
	0.9	4.897×10^{-8}
	0.95	1.713×10^{-10}

*Sanders, S.M., Kerrigan, W.J. and Albenesius, E.L. "Radiation Shielding for Sources of $^{170, 171}Tm$," USAEC Report DP 1158, E. I. duPont de Nemours & Co., Savannah River Laboratory, Aiken, South Carolina (1968).

dose rates.

A computer code was developed to calculate the uncollided dose rates by using the above equation. 19 cm was selected for the source to dose point distance. A conversion factor of 445 ± 22 curies per watt was used[22]. Twenty-two photon energy groups (Table 5-6) were used in the computation. The total dose rate was obtained by adjusting the uncollided dose rate for the scatter component by use of a build-up factor[23]. In these calculations, a build-up factor for an infinite homogeneous medium was assumed because the analysis of Compton scattering for a finite medium is very complex and was beyond the scope of this program.

To extend total theoretical dose rates from 19 cm to 100 cm, the inverse square law was used.

5.4 COMPARISON OF RESULTS

The experimental results differed from the analytical predictions in two ways. One, the theoretical dose rates were generally greater for a given source to-dose-point distance than the actual dose rates, and two, the measured dose rates at 100 cm were not those expected if the inverse square law were controlling.

The differences between predicted and experimental data were generally outside the experimental error ± 9% and were largely due to the use of B_∞ in the calculations of predicted dose rate. Accuracy in obtaining the value of the build-up factor was difficult because data to assess B_∞ for energies less than 0.5 Mev was not available nor was data for $\mu t < 1$. Values of B_∞ at these energies were obtained by extrapolation from data existing for values greater than 0.5 Mev. Extrapolation for lead, tungsten and uranium was relatively easy as the shape of the curves allows extensions with a minimum of uncertainty; however, extrapolation for aluminum and stainless steel was very difficult and whatever the shape chosen it carried a high degree of uncertainty. The value of B_∞ used then, carried a degree of uncertainty whose magnitude was a factor of the shielding material.

The total dose rates generated were overestimated by 10-20% for lead, tungsten and depleted uranium and by as much as 50% for aluminum and stainless steel.

The second difference observed was the departure from the inverse square law. The dose rates obtained from an unshielded source followed well the $1/r^2$ relationship and therefore, the difference must lie with the absorber.

The reasons for the deviation can be seen by again considering the scattered component of the dose rate. In the calculation of total dose rate, a build-up factor for infinite medium (B_∞) had been used. This B_∞ was obtained by assuming that both the radiation source and the dose point were imbedded in an infinite homogeneous medium. For the 19 cm geometry, the dose point was very close to the shield surface (~ 2 to 3 cm), while for 100 cm geometry, the separation distance between the shield surface and the dose point was approximately 80 cm. The solid angle subtended by the detector was nearly 2π for 19 cm geometry while it was much smaller for the 100 cm geometry. Therefore, compared to the 100 cm geometry, the 19 cm geometry more closely approximated the infinite medium case. Consequently, B_∞ is more applicable to dose points located close to the shield surface. If B_∞ were applied to a dose point far away from the shield surface, it would overestimate the total dose. The degree of overestimation would depend on the shielding material and its thickness, or more specifically, that scattering as seen at 100 cm would be a different case than scattering seen at 19 cm. Because of the complexity of the problem, analytical evaluation was difficult. To extend the total dose rate correctly from 19 cm to 100 cm, experimental ratios (D_{100}/D_{19}) have to be used. Figures 5-3 through 5-7 present the corrected theoretical data. For practical shielding design, this overestimation increases the margin of safety.

5.5 PREDICTED DOSE RATES FOR LARGE SOURCES

The sources used in this study had a maximum power of 20 watts. In actual fact, sources with power levels to the kilowatt range are feasible. The analytical methods used for

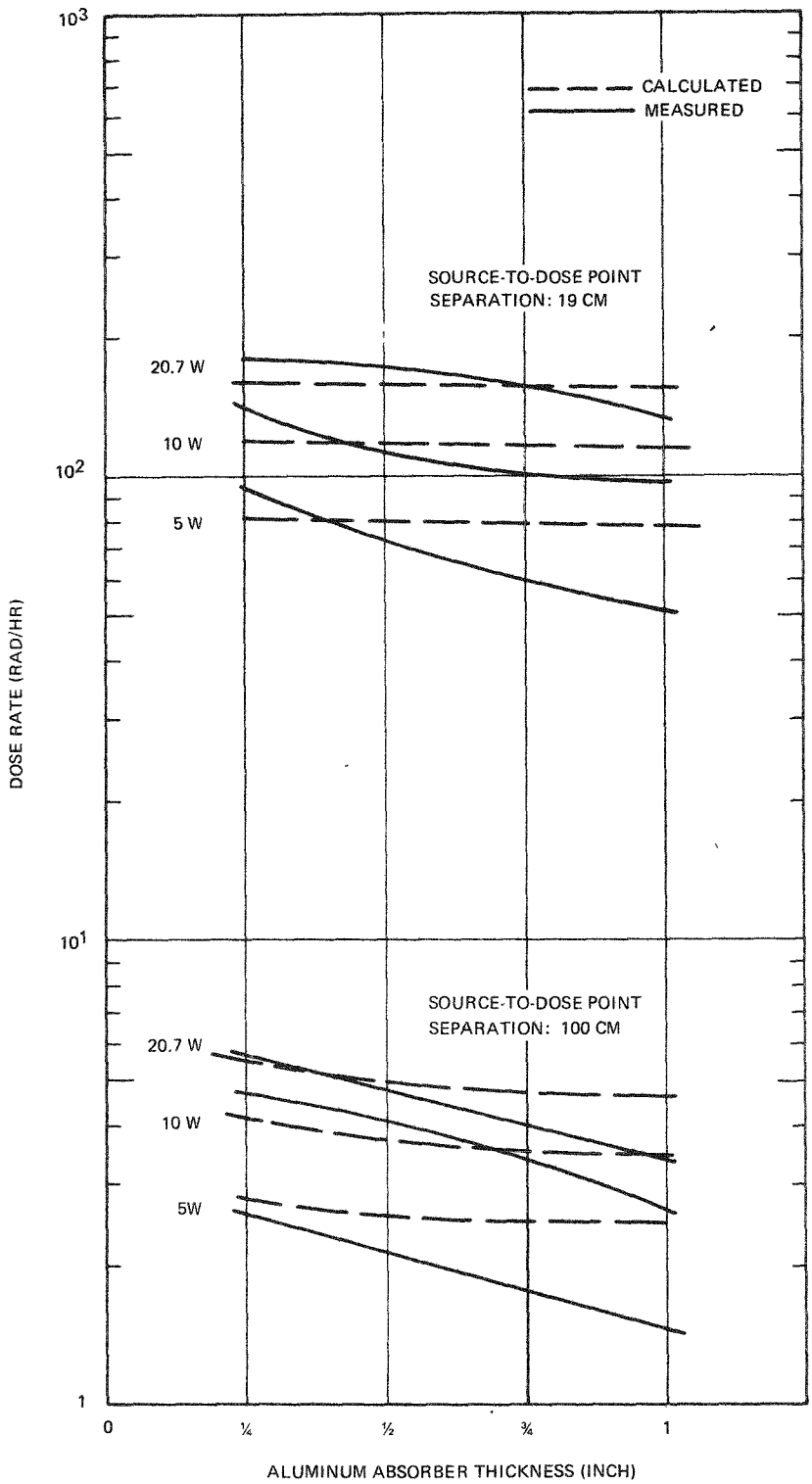

Figure 5-3. Comparison of Computed and Experimental Dose Rate Data for Thulium-170 using Aluminum Absorbers

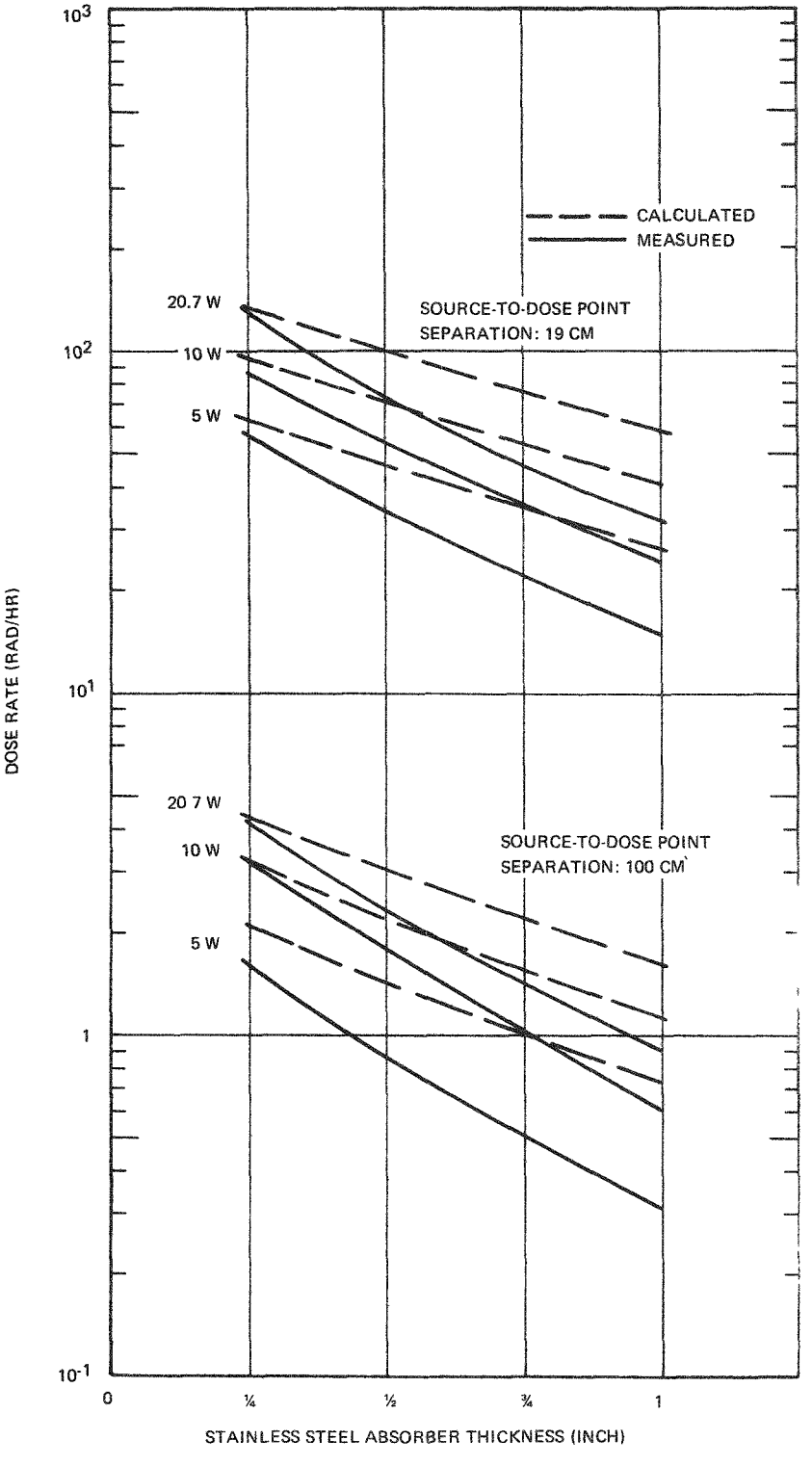

Figure 5-4. Comparison of Computed and Experimental Dose Rate Data for Thulium-170 using Stainless Steel Absorbers

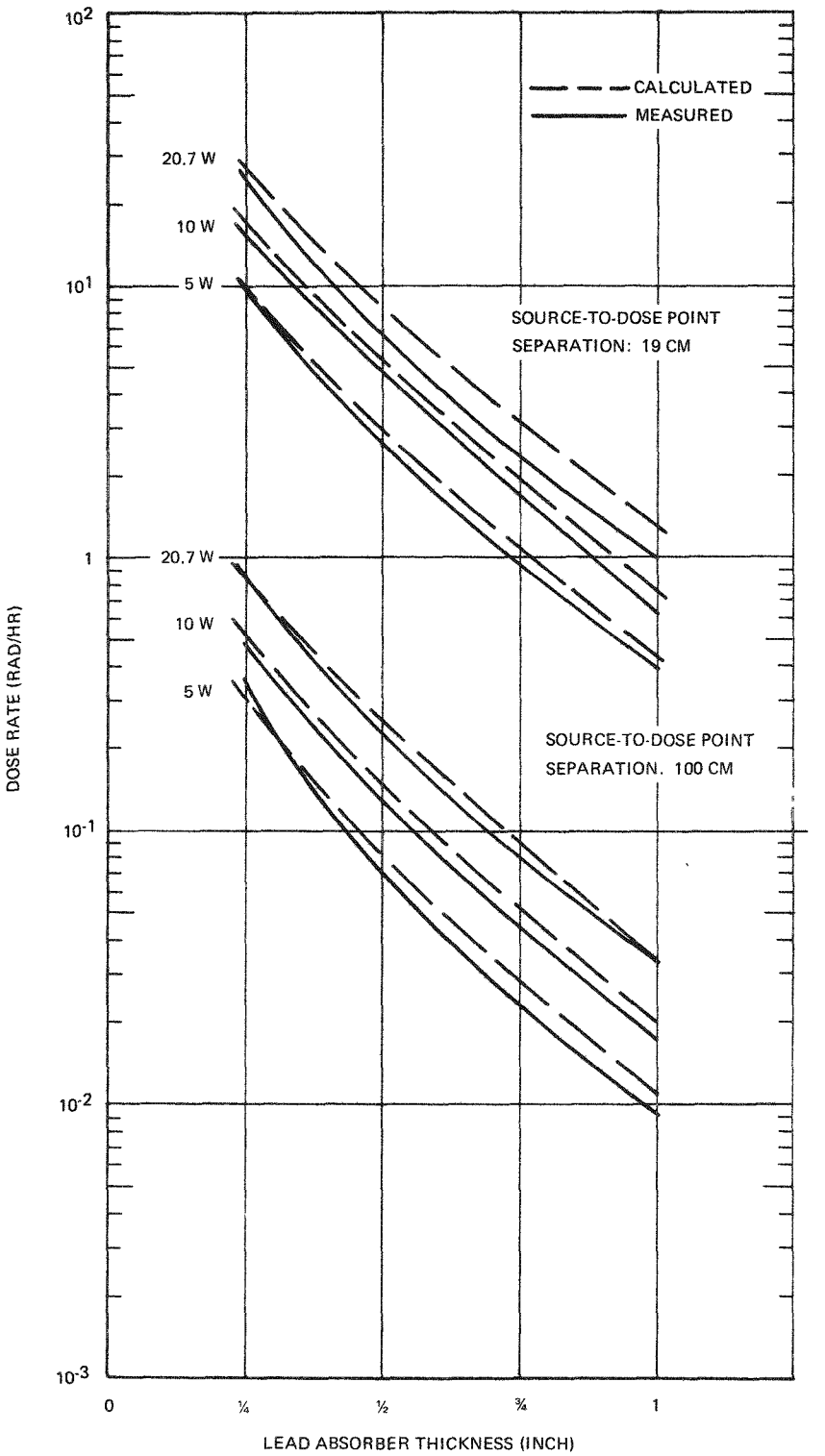

Figure 5-5. Comparison of Computed and Experimental Dose Rate Data for Thulium-170 using Lead Absorbers

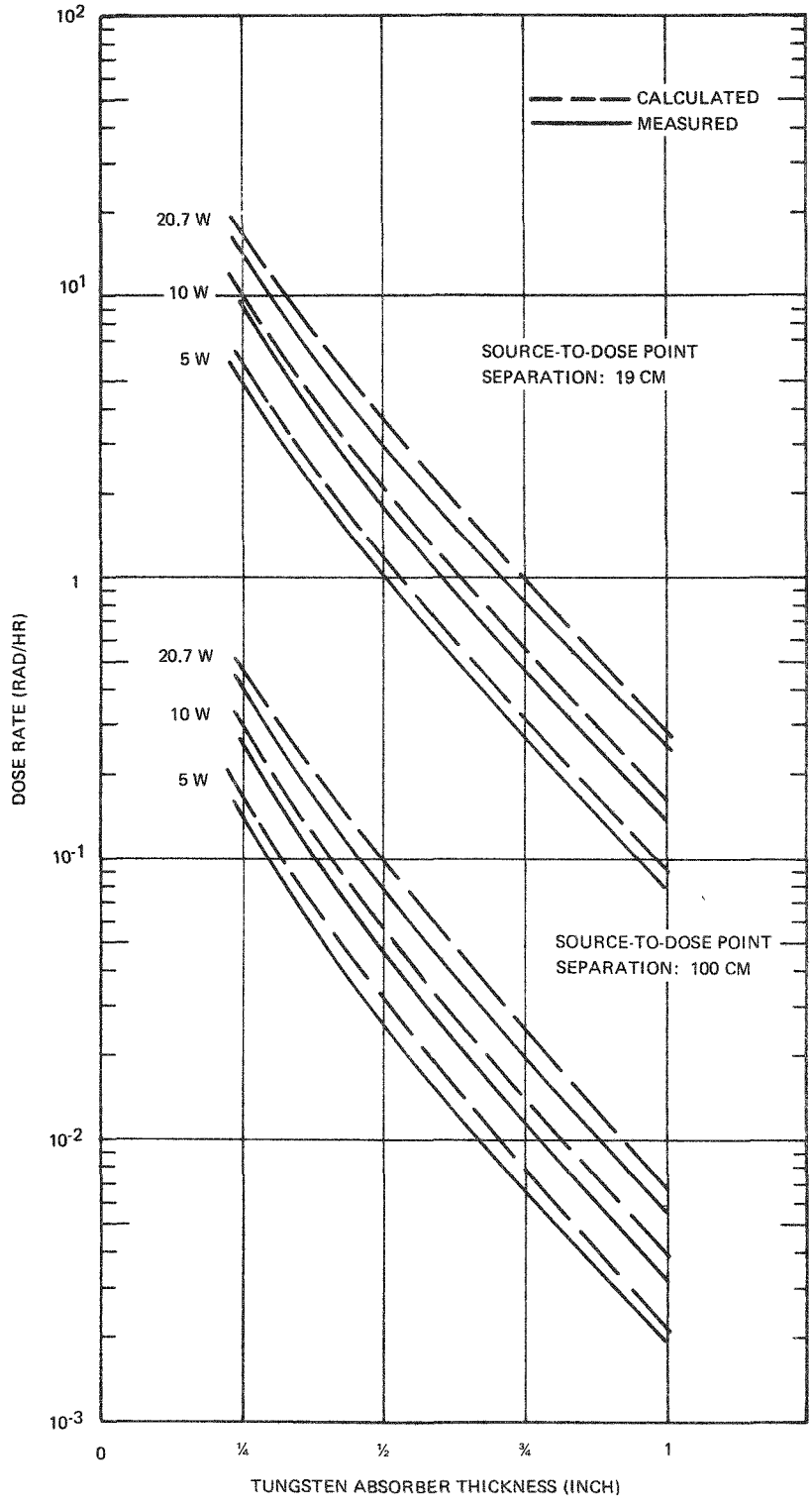

Figure 5-6. Comparison of Computed and Experimental Dose Rate Data for Thulium-170 using Tungsten Absorbers

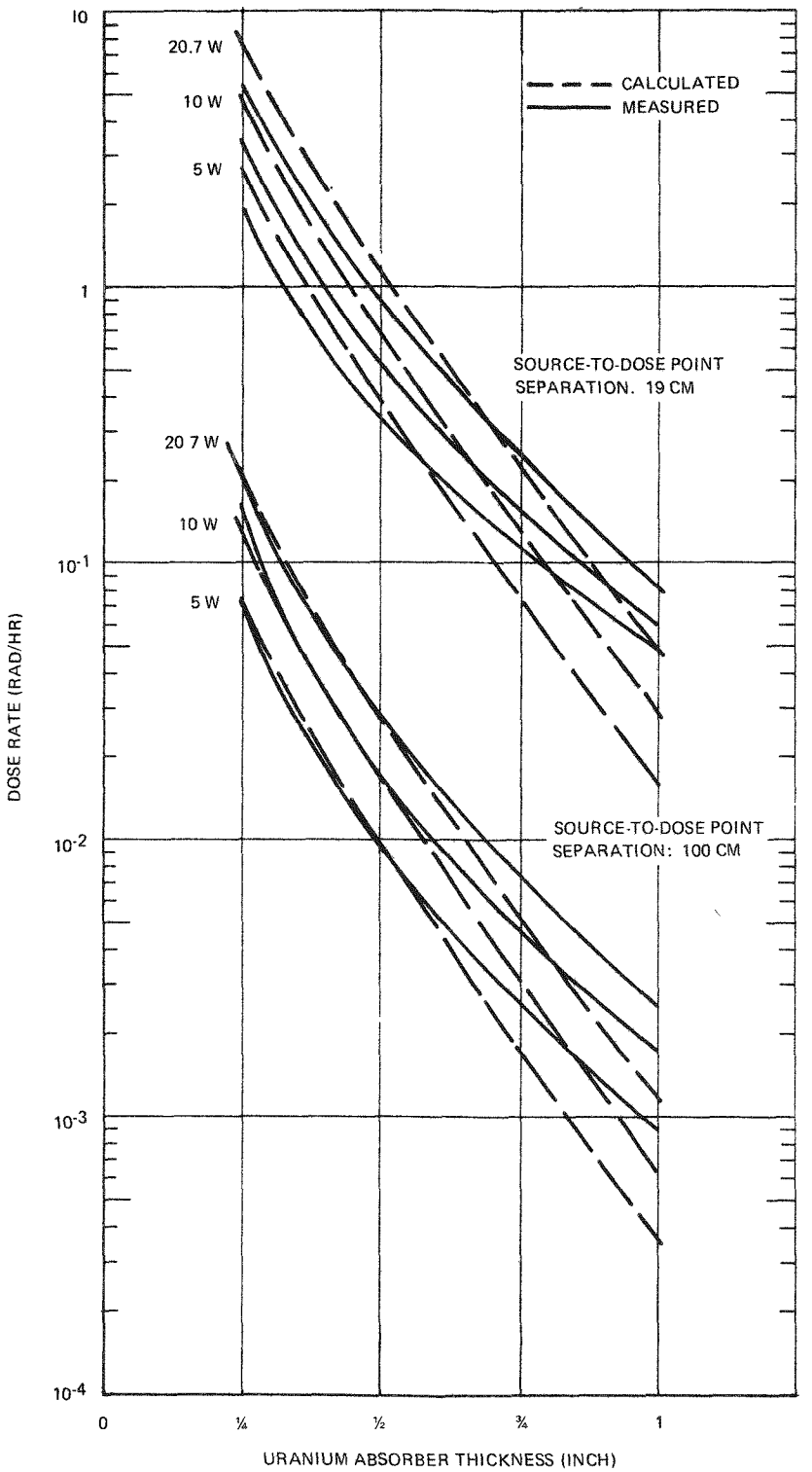

Figure 5-7. Comparison of Computed and Experimental Dose Rate Data for Thulium-170 using Uranium Absorbers

predicting doses from 20-watt sources through various absorbers can be applied to large scale sources. Calculations, however, must account for additional self attenuation and should be made on the basis of twenty-two energy groups as calculated dose rates will be high by as much as a factor of two if as few as four groups are used. The recommended buildup factor value for this calculation is B_∞. Even though this will overestimate the dose rate by 10-20% for lead, tungsten and depleted uranium, it results in only a 2-3% overestimate in shielding thickness (based on a 1 kilowatt thulium-170 source). This margin is conservative and is desirable because an uncertainty of 3-5% exists in the value of the absorption coefficients.

From this analysis, it can be concluded that methods developed for this study can be reliably applied to predicting dose rates from large scale sources (kilowatts) through lead, tungsten and depleted uranium shielding materials provided the geometry does not radically change.

5.6 CONCLUSIONS

Analytical techniques are available to predict axial dose rates from 5, 10 and 20.7-watt Tm_2O_3 sources at two different source-to-dose-point distances (19 and 100 cm). Five different absorber materials (aluminum, stainless steel, lead, tungsten and depleted uranium) of three different thicknesses (¼, ½ and 1") were used. Experimental data was obtained by thermoluminescent dosimetry techniques with an overall uncertainty of ± 9%.

Comparison of results shows a wide range of predicted-to-measured dose rates. The range is dependent on source-to-dose-point distance and on absorber material, and is largely attributable to the assumption of an infinite medium buildup factor. Predicted-to-measured dose rates at 19 cm varied from 20% (tungsten) to 83% (stainless steel).

Extension of analytical methods to kilowatt Tm_2O_3 sources

will provide dose rates that will fall within 20% of those actually experienced provided an infinite medium buildup factor is used in a twenty-two energy group computation.

A detailed presentation of this work may be found in Topical Report SNC-3693-4[4] entitled "Thulium-170 Oxide Heat Source Experimental and Analytical Radiation and Shielding Study."

SECTION 6
THULIUM-170 FUEL CAPSULE PARAMETRIC DESIGN

The fuel capsule parametric design study was performed during Phase I of the characterization study program (March-May 1968) with the purpose of providing sound technical guidelines on which to base subsequent experimental programs. Having preceded experimental data accummulation, it was necessary that the capsule parametric design study proceed on the basis of several assumptions:

- An infinitely long, cylindrical fuel capsule containing Tm_2O_3 in two different physical forms and in two different liner configurations.
- The melting point of Tm_2O_3 was 2300°C (4250°F).
- There were no solid-state transformations up to the melting point.
- There was encapsulant materials compatibility.
- Thermal conductivity of Tm_2O_3 fell within 1.5-3.0 B/hr-ft-°F.

Diameters of Tm_2O_3 wafers, maintained at 0.060 inch thickness, were varied between 0.6 and 3.0 inches. Radial temperature profiles were determined for Tm_2O_3 power densities ranging from 8 to 24 w/cc, and for fuel capsule surface temperatures ranging from 1000 to 2732°F (538-1500°C). Liner materials investigated were Hastelloy-X, Haynes-25, T-222, tungsten, platinum and molybdenum.

Experimental data now having been acquired respecting each of these parameters, it is appropriate to assess the impact of

experimental results on analytic results published in the Fuel Capsule Parametric Design Study[3].

6.1 MELTING POINT

For purposes of the Parametric Design Study, the Tm_2O_3 centerline melt temperature was identified as a limiting condition and melt temperature was assumed to be 4250°F. In performance of Phase Diagram experiments to obtain the melt point of thulia, it was determined that the Tm_2O_3 melt point is 4172°F (2301°C)[2], that Tm_2O_3 and its decay product Yb_2O_3 are mutually soluble in all mixture ratios, and that the Yb_2O_3 melt point is 4211°F (2328°C). These temperatures, 4172 and 4221°F very closely approximate the 4250°F temperature with respect to which conclusions were drawn in the Parametric Design report, therefore, validate the melt point assumptions.

6.2 SOLID-STATE PHASE TRANSFORMATIONS

Radial thermal profiles in fuel capsules are a sensitive function of the radiation gap width between fuel and liner. Gap width is generally kept to that minimum consistent with the thermal coefficients of expansion of liner and fuel form in the temperature range of operation and consistent with the manufacturing tolerances which can be maintained. Rarely, but occasionally, gap width, hence thermal radial profile, is also a function of fuel form crystalline structure. At the outset of the Parametric Design Study, it was recognized that thulium metal exists as a close-packed, hexagonal structure but upon decay shifts to face-centered cubic ytterbium with consequent development of internal stress and a change in fuel form physical dimensions. A question existed, therefore, as to whether Tm_2O_3 and Yb_2O_3 would remain cubic throughout the temperature range, ambient to the melt point. In the Parametric Design Study, retention of the cubic form was assumed. In determination of the Tm_2O_3 - Yb_2O_3 phase diagram, it was confirmed that the cubic structure was retained to the melt point; ergo, the fuel capsule parametric design study, in which gap width was assumed to be only a function of thermal coefficients of expansion and manufacturing tolerances, was validated.

6.3 COMPATIBILITY

The fuel capsule parametric study considered containment materials to include Hastelloy-X, Haynes - 25, T-222, tungsten, platinum and molybdenum on the basis that these had each previously proved useful radioisotope encapsulants. In Phases II and III of the program, containment of Tm_2O_3 and Tm_2O_3 - Yb_2O_3 mixtures was demonstrated to 5 half lives (10,000 hours) with Hastelloy-X, Hastelloy C-276, Haynes-25, T-111, tungsten, TZM and zirconium. Haynes-25 and Hastelloy-X tests were conducted to 1000°C; T-111 to 1600°C; tungsten and TZM to 2000°C. The fuel capsule parametric design study was validated respecting Hastelloy C-276, Haynes-25 and tungsten by actual test, and was qualitatively validated respecting T-222 and molybdenum by the T-111 and TZM tests, respectively.

6.4 THERMAL CONDUCTIVITY

In the absence of Tm_2O_3 thermal conductivity data at the time of the fuel capsule parametric design study, it was decided to present results on the basis that thermal conductivity, when measured, would be found to lie between 1.5 B/hr-ft-°F (0.026 w/cm-°C) and 3.0 B/hr-ft-°F (0.052 w/cm-°C). Hence, two sets of fuel capsule thermal profiles were developed; one on the assumption of 0.026 w/cm-°C and the other on the assumption of 0.052 w/cm-°C[3]. Figure 6-1[24] presents thermal conductivity test data acquired subsequent to the parametric design study.

The temperature range of interest was 1000°F (538°C) to 4172°F (2300°C); corresponding thermal conductivities were 0.037 w/cm-°C and 0.01 w/cm-°C (extrapolation). These bracketed well the results presented at an assumed thermal conductivity of 0.026 w/cm-°C (1.5 B/hr-ft-°F) and required a positive correction of approximately 150°C on all results shown at 3.0 B/hr-ft-°F; i.e., centerline temperatures based on K = 3.0 B/hr-ft-°F should be so adjusted. As a generalization, it can be said that capsule internal temperatures would be lower than depicted graphically[3] for all those cases examined where K= 1.5 B/hr-ft-°F and fuel capsule surface temperature

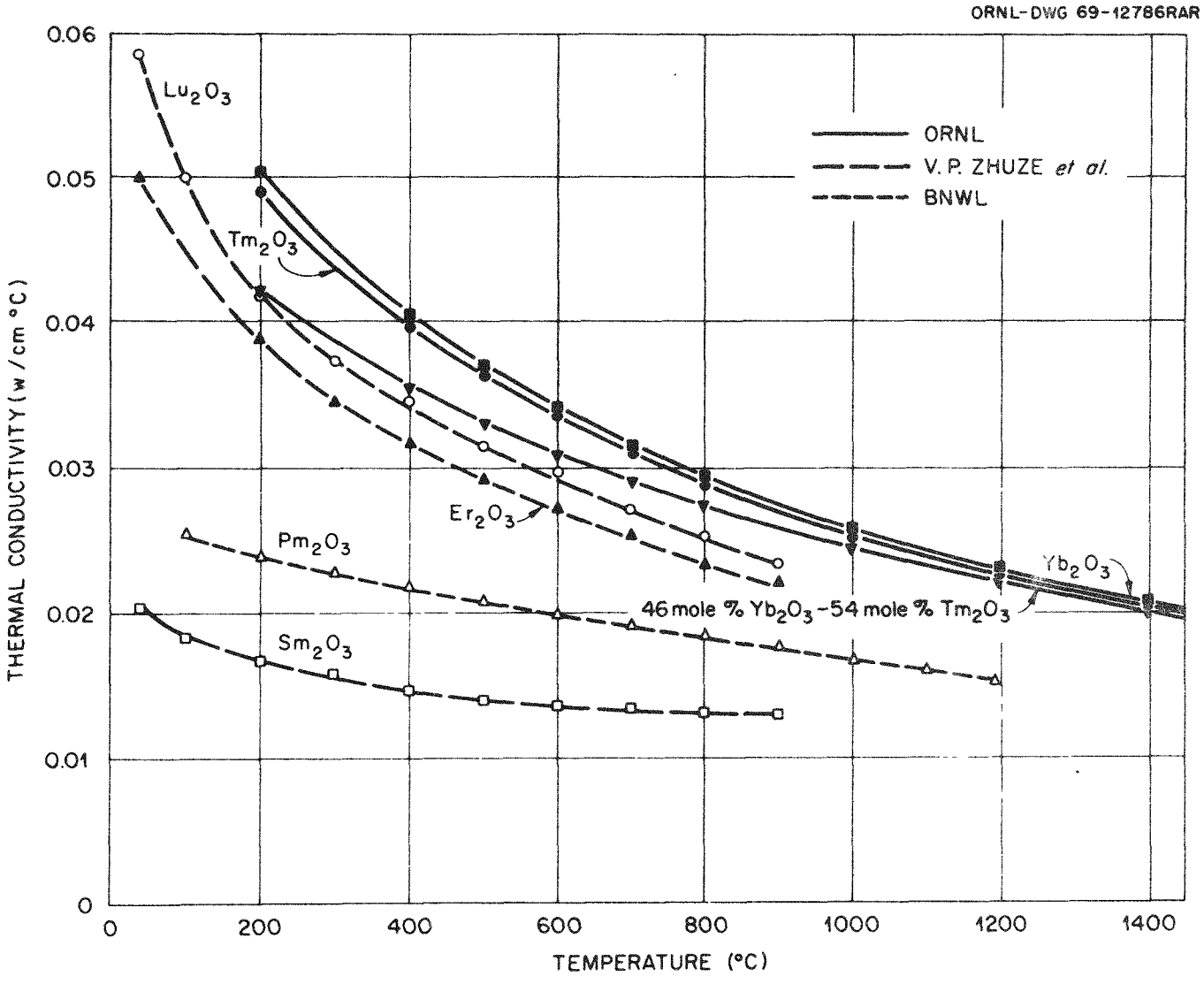

Figure 6-1. Thermal Conductivity versus Temperature for Tm_2O_3, Yb_2O_3, 46 Mole % Yb_2O_3 to 54 Mole % Tm_2O_3, and Other Rare-Earth Oxides [24]

equaled 1000°F; profiles were approximately correct where K = 1.5 B/hr-ft-°F and capsule surface temperature equaled 1500°F; and, capsule internal temperatures would be higher than depicted graphically[3] for those cases where K = 1.5 B/hr-ft-°F and capsule surface temperature were 2000°F.

6.5 CONCLUSIONS

Experimental evidence generated subsequent to preparation of the Fuel Capsule Parametric Design Study respecting thulia melt point, encapsulant compatibility and solid-state phase transformation, validate assumptions upon which the Parametric Design Study was performed. Experimental evidence respecting thermal conductivity required adjustment of thermal profiles presented in cases where K = 3.0 B/hr-ft-°F and conclusions drawn with respect thereto in the summary tables. Tables 6.1 - 6.6 of this report reflect these adjustments with "yes" indicating a viable set of conditions. Remaining profiles and conclusions drawn respecting them in Tables 6-1 through 6-3[3], were nominally correct as discussed in the foregoing paragraph.

For future fuel capsule design, the thermal profiles generated should be replotted based on the experimental thermal conductivity data now available. Consideration also should be given acquisition of experimental thermal conductivity data beyond those determined experimentally to date, as several applications exist wherein either the surface temperature or the internal temperature exceeds 1400°C, the limit of experimental data at present. This is appropriate since encapsulant integrity has been proven for temperatures up to 2000°C for times to 10,000 hours. The evidence that Tm_2O_3 thermal conductivity is lower at high system design operating temperatures than was postulated has meaning respecting thulia applicability as follows:

- At high fuel capsule surface temperatures, individual capsules should be of lesser diameter for safe operation than is reflected by thermal profiles[3].

TABLE 6-1

Tm_2O_3 WAFERS INDIVIDUALLY ENCAPSULATED, HASTELLOY-X OR HAYNES -25

CAPSULE SURFACE TEMPERATURE: 1000°F

Thermal Conductivity K = 1.5 B/Hr-Ft-°F	Fill Gas: Argon			Fill Gas: Helium		
	Fuel Diameter, in.			Fuel Diameter, in.		
Power Densities, w/cc	0.6	1.8	3.0	0.6	1.8	3.0
8	yes	yes	no	yes	yes	no
16	yes	no	no	yes	yes	no
24	yes	no	no	yes	no	no
Thermal Conductivity K = 3.0 B/Hr-Ft-°F	**Fuel Diameter, in.**			**Fuel Diameter, in.**		
Power Densities, w/cc	**0.6**	**1.8**	**3.0**	**0.6**	**1.8**	**3.0**
8	yes	yes	no	yes	yes	no
16	yes	no	no	yes	yes	no
24	yes	no	no	yes	no	no

TABLE 6-2

Tm_2O_3 BULK ENCAPSULATED IN HASTELLOY-X OR HAYNES-25
CAPSULE SURFACE TEMPERATURE: 1000°F

Thermal Conductivity K = 1.5 B/Hr-Ft-°F	Fill Gas: Argon			Fill Gas: Helium		
	Fuel Diameter, in.			Fuel Diameter, in.		
Power Density, w/cc	0.6	1.8	3.0	0.6	1.8	3.0
8	yes	no	no	yes	yes	no
16	yes	no	no	yes	no	no
24	yes	no	no	yes	no	no
Thermal Conductivity K = 3.0 B/Hr-Ft-°F	**Fuel Diameter, in.**			**Fuel Diameter, in.**		
Power Density, w/cc	0.6	1.8	3.0	0.6	1.8	3.0
8	yes	no	no	yes	yes	no
16	yes	no	no	yes	no	no
24	yes	no	no	yes	no	no

TABLE 6-3

Tm_2O_3 WAFERS INDIVIDUALLY ENCAPSULATED, PLATINUM OR T-222
CAPSULE SURFACE TEMPERATURE: 1500°F

Thermal Conductivity K = 1.5 B/Hr-Ft-°F	Fill Gas: Argon			Fill Gas: Helium		
	Fuel Diameter, in.			Fuel Diameter, in.		
Power Density, w/cc	0.6	1.8	3.0	0.6	1.8	3.0
8	yes	yes	yes	yes	yes	yes
16	yes	yes	no	yes	yes	yes
24	yes	no	no	yes	yes	no
Thermal Conductivity K = 3.0 B/Hr-Ft-°F	**Fuel Diameter, in.**			**Fuel Diameter, in.**		
Power Density, w/cc	**0.6**	**1.8**	**3.0**	**0.6**	**1.8**	**3.0**
8	yes	yes	yes	yes	yes	yes
16	yes	yes	no	yes	yes	yes
24	yes	no	no	yes	yes	no

TABLE 6-4

Tm_2O_3 BULK ENCAPSULATED IN PLATINUM
CAPSULE SURFACE TEMPERATURE: 1500°F

Thermal Conductivity K = 1.5 B/Hr-Ft-°F	Fill Gas: Argon			Fill Gas: Helium		
	Fuel Diameter, in.			Fuel Diameter, in.		
Power Density, w/cc	0.6	1.8	3.0	0.6	1.8	3.0
8	yes	yes	no	yes	yes	no
16	yes	no	no	yes	no	no
24	yes	no	no	yes	no	no
Thermal Conductivity K = 3.0 B/Hr-Ft-°F	**Fuel Diameter, in.**			**Fuel Diameter, in.**		
Power Density, w/cc	**0.6**	**1.8**	**3.0**	**0.6**	**1.8**	**3.0**
8	yes	yes	no	yes	yes	no
16	yes	no	no	yes	no	no
24	yes	no	no	yes	no	no

TABLE 6-5

Tm_2O_3 WAFERS INDIVIDUALLY ENCAPSULATED, MOLYBDENUM OR TUNGSTEN
CAPSULE SURFACE TEMPERATURE: 2000°F

Thermal Conductivity K = 1.5 B/Hr-Ft-°F	Fill Gas: Argon			Fill Gas: Helium		
	Fuel Diameter, in.			Fuel Diameter, in.		
Power Density, w/cc	0.6	1.8	3.0	0.6	1.8	3.0
8	yes	yes	yes	yes	yes	yes
16	yes	yes	no	yes	yes	yes
24	yes	yes	no	yes	yes	no
Thermal Conductivity K = 3.0 B/Hr-Ft-°F	**Fuel Diameter, in.**			**Fuel Diameter, in.**		
Power Density, w/cc	0.6	1.8	3.0	0.6	1.8	3.0
8	yes	yes	yes	yes	yes	yes
16	yes	yes	no	yes	yes	yes
24	yes	yes	no	yes	yes	no

TABLE 6-6

Tm_2O_3 BULK ENCAPSULATED IN MOLYBDENUM, T-222, OR TUNGSTEN
CAPSULE SURFACE TEMPERATURE: 2000°F

Thermal Conductivity K = 1.5 B/Hr-Ft-°F	Fill Gas: Argon			Fill Gas: Helium		
	Fuel Diameter, in.			Fuel Diameter, in.		
Power Density, w/cc	0.6	1.8	3.0	0.6	1.8	3.0
8	yes	yes	no	yes	yes	no
16	yes	no	no	yes	no	no
24	yes	no	no	yes	no	no
Thermal Conductivity K = 3.0 B/Hr-Ft-°F	Fuel Diameter, in.			Fuel Diameter, in.		
Power Density, w/cc	0.6	1.8	3.0	0.6	1.8	3.0
8	yes	yes	no	yes	yes	no
16	yes	no	no	yes	no	no
24	yes	no	no	yes	no	no

- A valid very strong argument now exists for individual encapsulation of thulia wafers vis-a-vis application of bulk encapsulated material or microspheres. Figure 6-2 depicts the thermal profiles for individually encapsulated (Hastelloy-X) wafers and bulk encapsulated wafers assuming a surface temperature of 1000°F. The benefits in lower centerline temperature afforded by the multiple radial metallic paths for heat conduction to the fuel capsule surface are inherent in the individual encapsulated wafer approach and will prove essential to design of all relatively large diameter fuel capsules of high surface operating temperature.

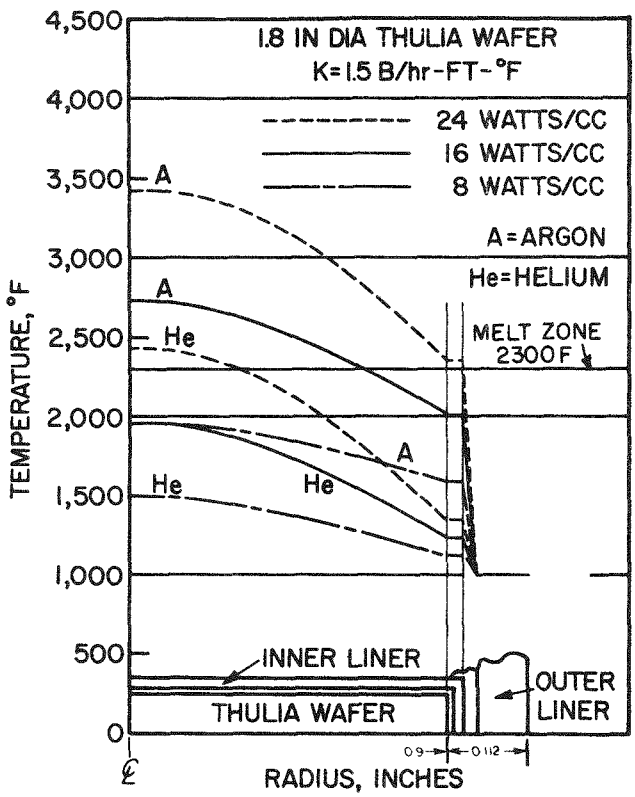

1.8 in. dia Thulia Wafer,
K = 1.5 B/hr-ft-°F

Individually Encapsulated

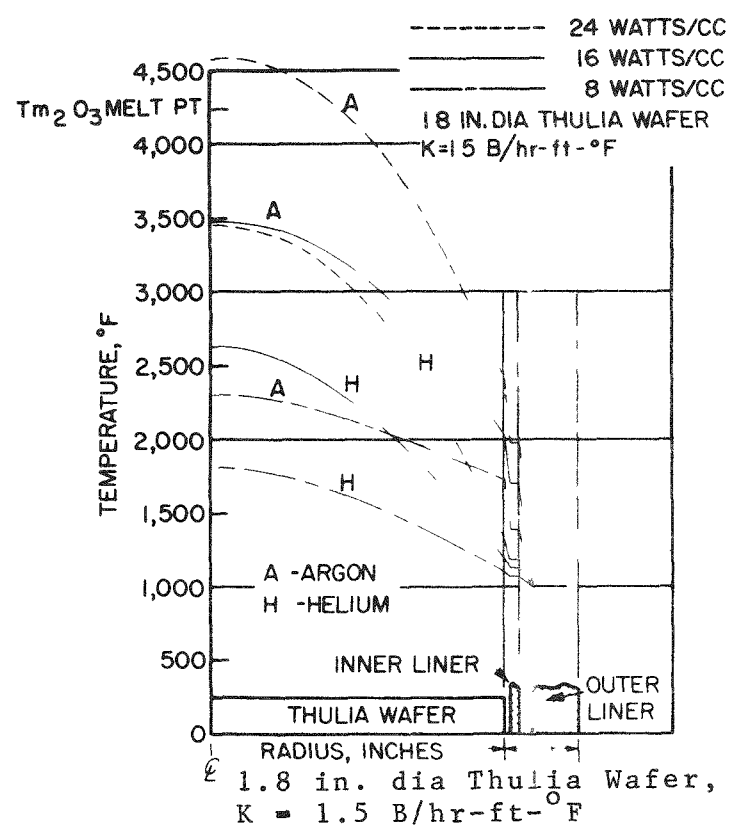

1.8 in. dia Thulia Wafer,
K = 1.5 B/hr-ft-°F

Bulk Encapsulated

Figure 6-2. Individually and Bulk Encapsulated Wafer Thermal Profiles, Surface Temperature 1000°F, Hastelloy-X Liners

SECTION 7
EVALUATION OF TEST SAMPLE PREPARATION PROCEDURE

The properties of ceramic powders used as starting materials for preparing sintered bodies largely determine the mechanical, thermal and chemical properties of the ceramic body. Several factors determine the quality of these starting materials, such as composition, purity, particle size and particle shape.

The size and shape of the particles have the greatest effect on the sintering properties. The particle size determines the amount of free surface energy available for the sintering process. For this study, the process developed at Savannah River Laboratories was designated as the basic procedure to produce a starting Tm_2O_3 powder with large surface area for sintering.

The approach consists of converting the "as received" oxide into a soluble form (nitrate) and reprecipitating the thulium or coprecipitating thulium and ytterbium as the hydroxide. Principally, experimental conditions are imposed such that very fine particle size material is obtained. After drying, precipitates are subsequently calcined in air to obtain the oxide and then ground to size (100 mesh) prior to adding binder for subsequent pressing. Further details of the procedure may be found in Part III of this report, "Procedures".

In our laboratory, the process through calcining produced a fine particulate white powder of several times the volume of the original "as received" oxide. Conversion efficiencies (oxide-to-oxide) for the relatively high cost starting material were

consistently better than 90%, and was considered an acceptable yield. In instances where Tm_2O_3/Yb_2O_3 mixed oxides were required, projection of existing rare earth oxide data indicated that thulium and ytterbium could be coprecipitated as hydroxides without segregation. Yields under these conditions also exceeded 90%.

Initial processing of the "as received" Tm_2O_3/Yb_2O_3 required a strong nitric acid treatment that leached silicon from the glassware to the extent of increasing silicon levels by an order of magnitude in the calcined powder. Since the hydroxide precipitation process is a scavenger, a poor impurity decontamination factor resulted. The higher silicon level could not be lowered by the process. To avoid introducing more impurities in subsequent preparations, plastic ware was used.

The impurity levels detected in the processed material were somewhat higher than those levels measured in the "as received" oxide. Emission spectrochemical analysis of samples representative of the process are shown in Table 7-1. These were the elements present in significant amounts. Since impurities may have coprecipitated with the thulium, a close control of impurities in reagents must be considered; impurities can give rise to a liquid phase during sintering and cause discontinuous grain growth and represent a potential reactant with the encapsulant.

Impurities may also result in situ as a result of incomplete chemical conversion. Investigation of calcination of plutonia has shown that residual carbon remains even after ignitions to 1000°C[25]. Keski and Smith[26] have also shown a similar behavior with "as received" thulium oxide as a result of incomplete oxalate-to-oxide conversion. The hydroxide process does have potential for introducing carbon residual through carbonate formation in the initial caustic solutions and in the subsequent washing operations. Insofar as carbon may be difficult to remove entirely, its presence represented a potential problem because its behavioral pattern was not known.

TABLE 7-1

SEMIQUANTITATIVE SPECTROCHEMICAL ANALYSIS

Lot or Batch No.	Sample	Concentration (ppm) Si	Al	Mg	Ca	Fe	Mn
Tm-201-0	Tm_2O_3 powder	200	30	10	100	100	ND <20
1A	100% Tm_2O_3 wafer	500	50	20	100	100	ND <20
6C	90% Tm_2O_3, 10% Yb_2O_3 wafer	300	50	20	100	100	ND <20
1F	70% Tm_2O_3, 30% Yb_2O_3 wafer	300	50	20	100	100	ND <20
1H	50% Tm_2O_3, 50% Yb_2O_3 wafer	300	100	20	100	100	20
1G	20% Tm_2O_3, 70% Yb_2O_3 wafer	300	100	20	100	300	20
1J	10% Tm_2O_3, 90% Yb_2O_3 wafer	300	100	20	100	300	20
1K	100% Yb_2O_3 wafer	200	80	20	200	200	10
Yb-100-0	Yb_2O_3 powder	50	10	10	100	200	10

NOTE: 1. ND = not detected

2. The limit of detection of Mn was lower in ytterbia than in thulia.

Using their process, SRL produced wafers having a nominal grain size of 5 - 10μ with densities of 95 - 97% of theoretical density when sintered in air at 1750°C. Wafers with densities to 96% of theoretical were obtained at Sanders when sintered in air at 1450°C. The grain size of these latter wafers were not resolvable with optical microscopy and therefore, were assumed to be less than about one micron.

This modified process was used to prepare all of the test samples for the compatibility studies and the phase diagram determination.

No difference in sintered wafer quality could be detected between wafers prepared from 100% Tm_2O_3 and those containing Yb_2O_3 except for slight differences in color. Table 7-2 presents the x-ray fluorescence analysis data for a series of Tm_2O_3/Yb_2O_3 compositions. The results indicate that the coprecipitation technique can reproducibly provide powder samples whose composition is reasonably close to that desired.

The mixed oxides were prepared to simulate thulium oxide fuel samples that had experienced nominal decay of Tm-170 to Yb-170. Even though the decay product was artifically induced, the properties, i.e., composition, purity, grain size, etc., were the same as those of the 100% Tm_2O_3 preparations. Therefore, the mixed oxides, prepared were considered a simulant of decayed product from the process point of view.

In summary, the process developed, can, with some quality control, reproducibly provide thulium oxide and thulium/ytterbium oxide wafers with sintered densities to 96% of theoretical. The conversion efficiencies (oxide-to-oxide) were consistently at an acceptable 90% level or better. Coprecipitation was used to prepare the mixed oxide starting powders. The sintered wafers were homogeneous and provided a quality simulant of the radioactive fuel thereby adding to the credibility of the compatibility and phase diagram data.

The chemically reprocessed oxide does not provide any

TABLE 7-2

X-RAY FLUORESCENCE ANALYSIS

SNC Batch No.	Nominal Composition		Analyzed Composition	
	Tm	Yb	Tm	Yb
1A	100	0	100	0
6C	90	10	88.6	11.4
1F	70	30	69.5	30.5
1H	50	50	49.2	50.8
1G	30	70	29.3	70.7
1J	10	90	11.1	88.9
1K	0	100	0	100

improvement in purity over the "as received" oxide. Impurities present a potential problem in that their behavioral pattern is unknown. It is recommended that other processes be studied that may be capable of providing a lower impurity level product of equally high ceramic quality.

SECTION 8
REFERENCES

1. R. W. Anderson, Compatibility Study of Containment Materials for Thulium Oxide, USAEC Report, SNC-3693-1, Sanders Nuclear Corporation, Nashua, N. H. (1970).

2. C. A. Nelson, R. W. Anderson and W. J. Fretague, Phase Diagram Determination of the Tm_2O_3 - Yb_2O_3 System, USAEC Report, SNC-3693-2, Sanders Nuclear Corporation, Nashua, N. H. (1970).

3. N. H. DesChamps, C. R. Fink and C. A. Nelson, Thulium Oxide Fuel Characterization Study (Thulium-170 Fueled Capsule Parametric Design), USAEC Report, SNC-3693-3, Sanders Nuclear Corporation, Nashua, N. H. (1970).

4. A. Tse and C. A. Nelson, Thulium-170 Oxide Heat Source Experimental and Analytical Radiation and Shielding Study, USAEC Report, SNC-3693-4, Sanders Nuclear Corporation, Nashua, N. H. (1970).

5. R. W. Anderson, Sanders Nuclear Internal Communication, July 1969.

6. Material furnished courtesy of S. J. Schneider, National Bureau of Standards.

7. S. J. Schneider and C. L. McDaniel, "Effect of Environment Upon the Melting Point of Al_2O_3," Journal of Research of the National Bureau of Standards, A. Physics and Chemistry, 71A, No. 4 (July - August, 1967).

8. P. K. Smith, "High Temperature Stability of Thulium Oxide," USAEC Report DP-116, E. I. duPont de Nemours & Co., Savannah River Laboratory, Aiken, S. C. (1967).

9. Private Communication, J. K. Poggenburg, Isotopes Development Center, Oak Ridge National Laboratories, Oak Ridge, Tennessee.

10. L. Eyring, H. Eick, paper presented at a Symposium on Rare Earth Chemistry at 17th Midwest Regional Meeting of American Chemical Society, Ames, Iowa (November 1956).

11. Ch. de Rohden, "Metaux et Composes des Terres Rares," Annales des Mines, 63-76 (1963).

12. V. M. Goldschmidt, F. Ulrich and T. Barth, "Geochemical Distribution of the Elements, Pt IV. 'On the Crystal Structure of the Oxides of the Rare Earth Metals'," Skrifte Norske Videnskap-Akad, Oslo I. Mat. Naturu Kl. No. 5 (1925).

13. Von G. Brauer and H. Gradinger, Z. Anorg. Allgem. Chem, 276 209 - 226 (1954).

14. E. Staritsky, Anal Chem, 28, 2023-2024 (1956).

15. R. S. Roth and S. J. Schneider, J. Res NBS. 64A, 309-316 (1960).

16. I. Warshaw and R. Roy, J. Phys Chem, 65, 2048-51 (1961).

17. M. Föex and J. P. Traverse, "High Temperature Study of the Allotropic Transformations of the Sesquioxides of Ytterbia, Erbium and Thulium," Compt. Rend Acad. Sci. Paris, T. 261, Gr. 8, 2090-93 (September 27, 1965) (In French).

18. See Part III, "Procedures."

19. Arnold, E. D., "Handbook of Shielding Requirements and Radiation Characteristics of Isotopic Power Sources for Terrestrial, Marine, and Space Applications," USAEC Report ORNL-3576, Oak Ridge National Laboratory, Oak Ridge, Tennessee (1964).

20. Rockwell, T., III., "Reactor Shielding Design Manual," D. Van Nostrand Co., Inc. New York (1959).

21. "Nuclear Data Sheets," Academic Press, New York (1966).

22. Cornman, W. R., "Production of Tm-170," USAEC Report DP-1052, E. I. duPont de Nemours and Co., Savannah River Laboratory, Aiken, S. C. (secret) (1967).

23. Goldstein, Herbert and J. Ernest Wilkins, Jr., "Calculations of the Penetration of Gamma Rays," NDA 15C-41; Nuclear Development Associates, Inc., Whiteplains, N. Y. (June 1954).

24. E. Lamb, ORNL Isotopic Power Fuels Quarterly Report for Period Ending March 31, 1970, USAEC Report, ORNL-4567, Union Carbide Corporation, Oak Ridge National Laboratories, Oak Ridge, Tennessee, p. 15-17 (1970).

25. B. Cina, "Some Decomposition Effects in PuO_2 on Sintering," Journal of Nuclear Materials, 9, No. 1 p. 87 - 88 (1963).

26. J. R. Keski and P. K. Smith, Fabrication and Irradiation Behavior of Thulium Sesquioxide, USAEC Report, DP-MS-68-28, E. I. duPont de Nemours & Co., Savannah River Laboratory, Aiken, S. C. (1968).